UNIVERSIDAD DE INVESTIGACIÓN DE

TECNOLOGÍA EXPERIMENTAL YACHAY

Escuela de Ciencias Químicas e Ingeniería

TÍTULO: DESIGN AND OPTIMIZATION OF A METHODOLOGY TO OBTAIN CELLULOSE AND CRYSTALLINE NANOCELLULOSE FROM OIL PALM EMPTY FRUIT BUNCH

Trabajo de integración curricular presentado como requisito

para la obtención del título de Químico

Autor:

Rochina Núñez Daniela Gisell

Tutor:

MSc. De Lima Eljuri Lola María

PhD. Caetano Sousa Manuel

Urcuquí, octubre 2021

SECRETARÍA GENERAL
(Vicerrectorado Académico/Cancillería)
ESCUELA DE CIENCIAS QUÍMICAS E INGENIERÍA
CARRERA DE QUÍMICA
ACTA DE DEFENSA No. UITEY-CHE-2022-00009-AD

A los 14 días del mes de enero de 2022, a las 15:00 horas, de manera virtual mediante videoconferencia, y ante el Tribunal Calificador, integrado por los docentes:

Presidente Tribunal de Defensa	Dra. MICHELL URIBE, ROSE MARY RITA , Ph.D.
Miembro No Tutor	Dr. TAFUR GUISAO, JUAN PABLO , Ph.D.
Tutor	Mgs. DE LIMA ELJURI, LOLA MARIA

El(la) señor(ita) estudiante **ROCHINA NUÑEZ, DANIELA GISELL**, con cédula de identidad No. **1718540782**, de la **ESCUELA DE CIENCIAS QUÍMICAS E INGENIERÍA**, de la Carrera de **QUÍMICA**, aprobada por el Consejo de Educación Superior (CES), mediante Resolución **RPC-SO-39-No.456-2014**, realiza a través de videoconferencia, la sustentación de su trabajo de titulación denominado: **Design and optimization of a methodology to obtain cellulose and crystalline nanocellulose from oil palm empty fruit bunch**, previa a la obtención del título de **QUÍMICO/A**.

El citado trabajo de titulación, fue debidamente aprobado por el(los) docente(s):

Tutor	Mgs. DE LIMA ELJURI, LOLA MARIA

Y recibió las observaciones de los otros miembros del Tribunal Calificador, las mismas que han sido incorporadas por el(la) estudiante.

Previamente cumplidos los requisitos legales y reglamentarios, el trabajo de titulación fue sustentado por el(la) estudiante y examinado por los miembros del Tribunal Calificador. Escuchada la sustentación del trabajo de titulación a través de videoconferencia, que integró la exposición de el(la) estudiante sobre el contenido de la misma y las preguntas formuladas por los miembros del Tribunal, se califica la sustentación del trabajo de titulación con las siguientes calificaciones:

Tipo	Docente	Calificación
Tutor	Mgs. DE LIMA ELJURI, LOLA MARIA	10,0
Miembro Tribunal De Defensa	Dr. TAFUR GUISAO, JUAN PABLO , Ph.D.	9,8
Presidente Tribunal De Defensa	Dra. MICHELL URIBE, ROSE MARY RITA , Ph.D.	9,0

Lo que da un promedio de: **9.6 (Nueve punto Seis)**, sobre 10 (diez), equivalente a: **APROBADO**

Para constancia de lo actuado, firman los miembros del Tribunal Calificador, el/la estudiante y el/la secretario ad-hoc.

Certifico que *en cumplimiento del Decreto Ejecutivo 1017 de 16 de marzo de 2020, la defensa de trabajo de titulación (o examen de grado modalidad teórico práctica) se realizó vía virtual, por lo que las firmas de los miembros del Tribunal de Defensa de Grado, constan en forma digital.*

ROCHINA NUÑEZ, DANIELA GISELL
Estudiante

ROSE MARY RITA MICHELL URIBE
Firmado digitalmente por ROSE MARY RITA MICHELL URIBE
Fecha: 2022.01.19 12:09:51 -05'00'

Dra. MICHELL URIBE, ROSE MARY RITA , Ph.D.
Presidente Tribunal de Defensa

Mgs. DE LIMA ELJURI, LOLA MARIA
Tutor

Firmado electrónicamente por:
LOLA MARIA DE LIMA

Firmado digitalmente
por JUAN PABLO TAFUR
GUISAO
Fecha: 2022.01.15
10:35:13 -05'00'

Dr. TAFUR GUISAO, JUAN PABLO , Ph.D.
Miembro No Tutor

Firmado electrónicamente por:
**MARIELA
SOLEDAD YEPEZ
MERLO**

YEPEZ MERLO, MARIELA SOLEDAD
Secretario Ad-hoc

AUTORÍA

Yo, **DANIELA GISELL ROCHINA NÚÑEZ**, con cédula de identidad 1718540782, declaro que las ideas, juicios, valoraciones, interpretaciones, consultas bibliográficas, definiciones y conceptualizaciones expuestas en el presente trabajo; así cómo, los procedimientos y herramientas utilizadas en la investigación, son de absoluta responsabilidad de el/la autora (a) del trabajo de integración curricular. Así mismo, me acojo a los reglamentos internos de la Universidad de Investigación de Tecnología Experimental Yachay.

Urcuquí, octubre de 2021.

Daniela Gisell Rochina Núñez

CI:1718540782

AUTORIZACIÓN DE PUBLICACIÓN

Yo, **DANIELA GISELL ROCHINA NÚÑEZ**, con cédula de identidad 1718540782, cedo a la Universidad de Tecnología Experimental Yachay, los derechos de publicación de la presente obra, sin que deba haber un reconocimiento económico por este concepto. Declaro además que el texto del presente trabajo de titulación no podrá ser cedido a ninguna empresa editorial para su publicación u otros fines, sin contar previamente con la autorización escrita de la Universidad.

Asimismo, autorizo a la Universidad que realice la digitalización y publicación de este trabajo de integración curricular en el repositorio virtual, de conformidad a lo dispuesto en el Art. 144 de la Ley Orgánica de Educación Superior

Urcuquí, octubre de 2021.

Daniela Gisell Rochina Núñez

CI:1718540782

DEDICATION

This work is dedicated to my parents, Laura Lucía Núñez Hidalgo and Jorge Rodrigo Rochina, for their unconditional love, for all sacrifice and effort realized, for always supporting me and trusting in my abilities, for been an example of perseverance, for been the fundamental pillar in my life and help me in my academic development. They have been my greatest motivation to never give up. I love them.

To my brothers Daniel and Diego who have been a great support on whom I have always been able to count and to Sasha for being there.

Daniela Gisell Rochina Núñez

ACKNOWLEDGMENTS

To MSc. Lola De Lima, PhD. Manuel Caetano for the knowledge provided, for their contribution, dedication and advice to the development of this research. I deeply appreciate the trust they placed in me.

To PhD. Antonio Acosta for his support and advice in academic and personal situations.as well as besides being sources of inspiration

To the School of Chemical Sciences and Engineering of Yachay Tech University, especially my professors PhD. Edward Ávila, PhD. Sandra Bonilla, PhD. Vivian Morera and MSc. Ruth Oropeza for their contribution in my academical training.

To the School of Biological Sciences and Engineering of Yachay Tech University, for allowing me to use the labs.

To the School of Earth Sciences, Energy and Environment of Yachay Tech University, especially to professor Elizabeth Mariño, who facilitated the development of this research work.

To my friends of Yachay Tech, especially to Jorge Perea, Mishel Brito, Francisco Prócel and Alexander Tipán for all shared moments, for their support and unconditional friendship.

Finally, l thanks to all who have collaborated to make this possible.

RESUMEN

En el Ecuador, el racimo de frutas vacías de palma aceitera (OPEFB) es un residuo agrícola sin aprovechar. Para agregar valor a estos desechos, se propone la extracción de celulosa y nanocelulosa cristalina (CNC) a partir de estos. El objetivo principal de este trabajo fue establecer una metodología de hidrólisis ácida para la obtención de CNCs. Para evaluar la eficiencia de la hidrólisis del ácido fosfórico se realizaron 13 experimentos que estudiaron la influencia de las condiciones de reacción como la temperatura, la concentración de ácido, la proporción celulosa-ácido así como el tiempo de reacción. Para la caracterización de la celulosa OPEFB modificada, este trabajo se enfoca en espectroscopía de infrarrojos por transformada de Fourier - Reflectancia Total Atenuada (ATR-FTIR), espectroscopía de difracción de rayos X (XRD) y microscopía electrónica de barrido (SEM), que proporcionan información sobre la estructura química y la morfología de las muestras. Después de estas técnicas, se pudo asegurar que la celulosa y la CNC obtenidas no tenían señales de contenido de lignina o hemicelulosa. Las mejores condiciones de reacción para producir CNCs con alta cristalinidad se realizan a una concentración de ácido fosfórico al 70% en una proporción de 1: 100 g / mL llevada a cabo a temperatura ambiente durante largos períodos de tiempo. Estas condiciones aseguran una producción de rendimiento de 42,7% a 80,74% en dependencia del tiempo de hidrólisis. El % de cristalinidad para la nanocelulosa cristalina de OPEFB está en el rango [75,1% - 85,4%]. Para proponer una aplicación precisa, se realizaron pruebas de tracción en películas de celulosa modificada de OPEFB con quitosano para evaluar el comportamiento mecánico en películas con 2% en peso de contenido de celulosa. Las películas evaluadas presentan un módulo de Young más alto, esto significa que la celulosa OPEFB modificada mejora las propiedades mecánicas de las películas de quitosano, por lo que funciona bien como material de relleno amigable con el ambiente.

Palabras clave: Celulosa de OPEFB, CNCs, polimorfos de celulosa, cristalinidad.

ABSTRACT

In Ecuador, Oil Palm Empty Fruit Bunch (OPEFB) is an agricultural waste that is not harnessed. To add value to these wastes, the extraction of Cellulose and Crystalline Nanocellulose (CNC) is proposed from them. The main objective of this work was to establish a methodology of acid hydrolysis for the obtention of CNCs. In order to evaluate the efficiency of phosphoric acid hydrolysis were carried out 13 experiments that study the influence of reaction conditions such as temperature, acid concentration, ratio between cellulose and acid and reaction time. For the characterization of modified OPEFB cellulose this work focus on Attenuated Total Reflection Fourier-transform infrared spectroscopy, (ATR-FTIR), X-Ray Powder Diffraction Spectroscopy (XRD), and Scanning Electron Microscopy (SEM), that provides information about chemical structure, and morphology from samples. After this techniques, was possible ensure that cellulose and CNC obtained do not have signals of lignin or hemicellulose content. The best reaction conditions to produce CNC with high crystallinity are 70% phosphoric acid concentration in a ratio 1:100 g/mL at room temperature for long periods of time. This conditions ensure a yield production from 42.7% to 80.74% in dependence of hydrolysis time. The %crystallinity for OPEFB crystalline nanocellulose has in range [75.1% - 85.4%]. To propose an accurate application Tensile Test were performed on chitosan - modified OPEFB cellulose films to evaluate the mechanical behavior at films with 2% wt. cellulose content. The films that were evaluated present a higher Young's modulus this means the modified OPEFB cellulose improve the mechanicals properties of chitosan films so, well works like green filler.

ABBREVIATIONS AND ACRONYMS

OPEFB   Oil Palm Empty Fruit Bunch

CNC   Crystalline Nanocellulose

MFC   Microfibrillated cellulose

CC   Crystalline Cellulose

AC   Amorphous Cellulose

CH   Chitosan

PA   Phosphoric Acid

ATR-FTIR   Attenuated Total Reflectance-Transform Infrared Spectroscopy

XRD   X-ray Powder Diffraction

SEM   Scanning Electron Microscopy

TABLE OF CONTENTS

LIST OF FIGURES

LIST OF TABLES

LIST OF ANNEXES

1 INTRODUCTION-JUSTIFICATION

Agriculture is one of the bases on which the economy of Ecuador is supported. The oil palm in Ecuador has been characterized as a growing, stable and successful productive field. Nowadays, Ecuador ranks second in Latin America in the production of crude palm oil and is the sixth largest producer worldwide. Although agribusiness is the key to the Ecuadorian economy, it generates large amounts of solid waste that have negative effects on the environment. In the oil industry, the contamination generated in relation to the processing activities of the fresh fruit bunches of the oil palm are the palm kernel shell, the mesocarp fiber as well as the oil palm empty fruit bunch. Around the world, an increasing researching effort has been devoted to develop processes that make it possible to value this type of agro-industrial waste and in this way turn this threat to the environment into an opportunity. In Ecuador, the oil palm empty fruit bunch is used as fuel to supply energy to the extraction plant while another fraction is incorporated into the plantation as a source of fertilizers. Despite these uses, the waste generated could be exploited according to its properties and used for the production of value-added inputs such as cellulose, crystalline nanocellulose, among others. It is important to remark that these materials are imported to Ecuador due to there is no industry for cellulose in our country. Also in Ecuador there is not a policy of supporting sustainability so the environment impact it is getting bigger every day. Thus, low-cost alternative materials synthesized, with an efficient methodology that can be applied in the Ecuadorian industry along with the intent to promote environmental sustainability, has motivated this research work.

2 PROBLEM STATEMENT

There is a strong and direct relationship between the production of palm oil and Ecuadorian agricultural domestic product, which frames the need to strengthen agro-industrial processes that entail sustainable processes. The use of agricultural residues has many advantages. OPEFB is considered the cheapest natural fiber with good properties and exists abundantly in Ecuador. It has great potential as an alternative main raw material to substitute woody plants. In this study, we are interested in isolating Cellulose and Crystalline Nanocellulose (CNC) from oil palm empty fruit bunches (OPEFB) with a simple method. In this way we can take advantage of organic waste and develop new products with higher added value.

The implementation of an appropriate method to isolate CNCs with good performance and good crystallinity would open an unexplored industrial field in Ecuador. Not only does it help to remediate waste but also produces a new material with applications in many industry fields such as biomedical, pharmaceuticals, drug delivery, remediation, food, textile, electronic, electrochemical among others.

3 GENERAL AND SPECIFIC OBJECTIVES

3.1 General objective

Isolation of cellulose and crystalline nanocellulose by acid hydrolysis method using oil palm empty fruit bunch, and the development of a methodology can be applied in ecuadorian industry.

3.2 Specific objectives

- To study in detail, the extraction of highly crystalline, H_2O-insoluble cellulose nanomaterials from oil palm empty fruit bunch by phosphoric acid hydrolysis.
- To study the effect of hydrolysis conditions on yield and morphology.
- To examine the interrelations of the extracted materials based on the conditions process, yield and structure obtained.
- To determine the reproducibility of the hydrolysis, and to explore ways to optimize the yield of the extracted nanomaterials with unique chemical and morphological properties.
- To blend chitosan with the extracted material from OPEFB as a green film for improving properties.
- To test the mechanical properties of modified OPEFB cellulose on chitosan films.

4 THEORETICAL BACKGROUND

4.1 Agricultural Industry in Ecuador

Agriculture is a fundamental pillar of the Ecuadorian economy. The production matrix is based on the agricultural sector that contributes 8% to the total annual production of the country (Gross Domestic Product). For the agricultural Ecuadorian industry, one of the most exploited products is Elaeis guineensis that is the palm oil species from which most oil palm is extracted quantity. In Latin America, Ecuador is in the second country of oil palm production [1]. Due to the adaptability of the plant for tropical conditions is cultivated throughout the three regions of Ecuador. On the coast, we have the provinces of Esmeraldas, Santo Domingo de los Tsáchilas, Guayas, Los Ríos, and Manabí. In the Sierra region are Pichincha, Imbabura, Cotopaxi and Bolívar while in the Amazon region we have the provinces of Orellana and Sucumbíos These provinces have favorable conditions for the production of the plant that supplies oil [2]. In Ecuador, oil palm plantations have an annual production of 2,275,948 tons according to INEC data. The current status of oil palm cultivation do not include a valorization of the residues generated and also, there is not a policy of supporting sustainability with the preservation of the Amazonian region and native tropical forest of Ecuador [3].

4.2 Oil Palm Empty Fruit Bunch

After oil palm production, the oil palm empty fruit bunch (OPEFB) is considered an agricultural waste that is discarded and its potential has not been harnessed. The processing of oil palm for oil extraction generates an abundance of by-products, in **Figure 4-1** show in detailed residues from oil palm. This raw material is a non-wood fiber that has great potential due to its properties and has a very low cost [4]. The chemical composition of OPEFB include [43-65%] cellulose, [17-33%] hemicellulose, [68-86%] holocellulose, [13-37%] lignin, [60-66%] glucose and [1-6%] ashes content. Thus, it is a suitable alternative in generating regenerated cellulose products. This biomass is used as natural fertilizer, biodiesel production, packaging, nanomaterials, among others [5].
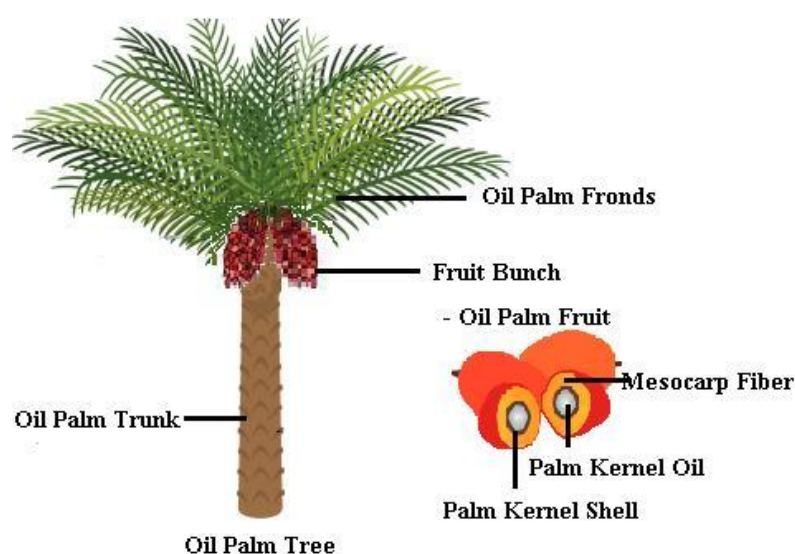
Figure 4-1. Agricultural wastes from oil palm

4.3   Cellulose

Cellulose is the most abundant biopolymer with exceptional characteristics such as renewability, biodegradability, biocompatibility and environmental friendliness. It can be obtained from different natural sources, like sugar palm, rice husk, cotton, wood, wheat, others plants, fruits, tunicate, algae, bacteria and fungi constituting the cell wall [6]. This macromolecule is formed from the repeating units of D-glucose, linked through glycosidic bonds (ß-1→4) that favor straight chains as shown in **Figure 4-2**. Cellulose forms a composite material with some polysaccharides like lignin and hemicellulose that constitute the primary structural matrix of plant tissues Its surface structure possesses abundant hydroxyl groups, therefore it can be easily functionalized by diverse chemical methods in order to enhance its physicochemical properties [7-8].
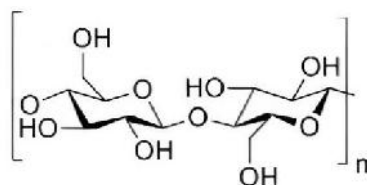
Figure 4-2. Molecular structure of cellulose repeat unit [8]

Cellulose has been of particular interest due to be considered a semi-flexible polymer. This means that its molecules have a tendency to form intramolecular that transform cellulose into a relatively stable polymer and provide the relative stiffness and intermolecular hydrogen bonds that allow a

tertiary fibrillar structure of high crystallinity of the molecule [9]. For crystalline cellulose has a representation in **Figure 4-3.** Cellulose has a semi-crystalline structure, this means that exist two regions, one region is crystalline (highly ordered) and other region is amorphous (less ordered) [10]. The crystallinity, is a measurable property, can be calculated from weight fraction of the crystalline regions. In order to describe the relative amount of crystalline material is used the crystallinity index (CI). Generally, in nature, the crystallinity degree is in the range of 40 to 70%, the rest is amorphous cellulose [11].
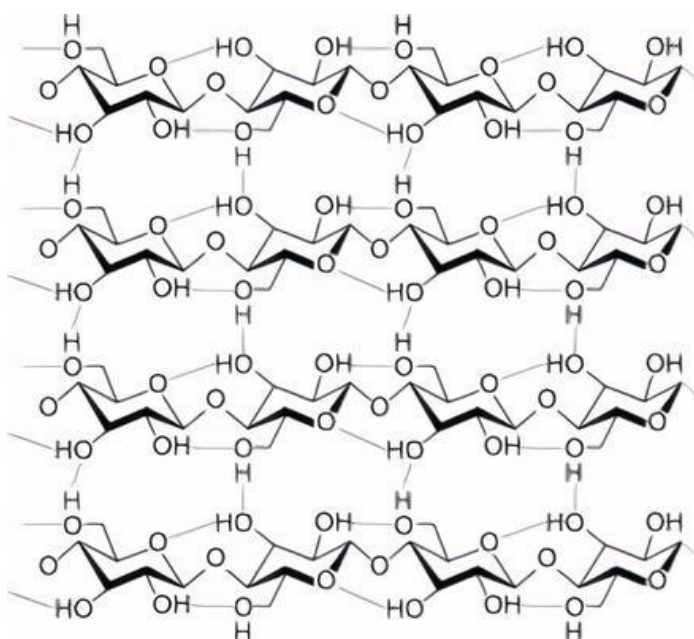
Figure 4-3. Structure of crystalline cellulose [10]

4.3.1   Cellulose Allomorphs

Cellulose chains presents differences in symmetry and chain geometry so, them can display different crystal packing. Exist four different polymorphs, known as cellulose I, II, III, IV. Cellulose polymorphs most common and present in plants is cellulose I or called native cellulose, and cellulose type II the difference between them is shown in **Figure 4-4**. Cellulose polymorph with a crystalline structure is known as cellulose I, when dissolved it crystallizes and passes to a more stable state known as cellulose II. Polymorphs III and IV are obtained after treatments with specific reagents [12-13].
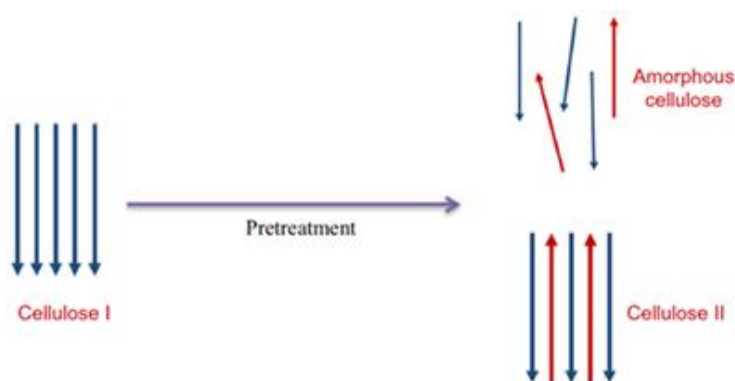
Figure 4-4. Most important cellulose allomorphs [13]

4.3.2 Processing of Cellulose

Nowadays, it pretends that chemical treatment will a green process that is way that various techniques have been explored to extract cellulose. The isolation of cellulose can be achieved in different ways but in the present work focus on chemical method. For a chemical pre-treatment, frequently used reagents are selected from oxidizing agents, alkali and acids due to the chemical reactions with raw material achieve for breaking the structure to degrade biomass and extract cellulose [14]. The theoretical framework of acid pre-treatment is removal of hemicellulose also are used to fractionate the components of lignocellulosic biomass while alkali pretreatment removal of lignin breaking the ester and glycosidic chains. As a result of both chemical treatments it is obtained a relatively pure cellulose [15].

In the case of employ acid reagents for pre-treatment is necessary take into account that reaction conditions. The efficiency of the treatment depends on critical parameters such as the type of acid, as well as the acid concentration, the ratio between biomass and acid (g/mL), also depends on temperature (usually high temperatures) and the time for acid treatment. All these parameters ensure a high yield of desired material. Among the most used chemicals are H_2SO_4, NHO_3, HCl and H_3PO_4. In the case of work with alkali reagents the efficiency also depends on the chemical nature, the alkali concentration as well as the ratio. The critical conditions for this pre-treatments are the reaction time because in order of the biomass type time will drag on. Also alkaline process operate at lower temperature that in acid conditions. The alkali reagent widely used are $NaOH$ and KOH [16-17].

4.4   Cellulose Applications

The cellulose has various application possibilities in different fields due to its huge availability worldwide, low cost, flexibility, easy processing, nontoxic, biodegradable and unique physicochemical properties [18]. Due to the formation of semicrystalline fibers cellulose has been used in papermaking field but nowadays, many studies have focused on cellulose-based materials renewability, versatility and functionality. That is why that cellulose is involved in many industry field for various applications like biomedical, pharmaceuticals, drug delivery, remediation, food, textile, electronic, electrochemical among others [19-21].

4.5   Crystalline Nanocellulose

When mention Cellulose Nano-Crystals (CNC) is refer to crystalline cellulose (highly ordered) in a scale of nanometers. At that scale based on it morphological structure is possible obtain different geometries for nanocellulose. A rod-like shape nanocrystals, filament-like long nanofibril (CNF) and sphere-like nanocellulose as example see **Figure 4-5** [22]. Based on exhaustive literature review about morphology of nanoparticles it can be stated that the average particle size for CNCs exhibit a length of 50–350 nm, respect to the width of 5–20 nm, and for aspect ratios of 5–30 nm. In contrast, a fibrillar particle morphology belong to CNFs and present a flexible structure. Their typical length is more than 1 μm, the average width is between 20–100 nm, and for it aspect ratio is 10–100 nm [23].
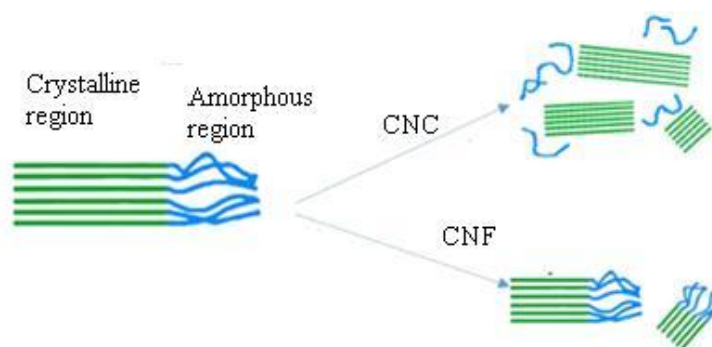
Figure 4-5. Different morphology for nanoparticles [24]

4.5.1   Processing of CNC

Exist different mechanisms to isolate cellulose nanocrystals like biological, mechanical, and chemical. In this section, explained the chemical method to isolate CNC is chemical that

encompasses an acid hydrolysis. This experimental procedure is widely used in the process of separation of CNCs from amorphous cellulose. The amorphous regions of cellulose must be hydrolyzed under certain conditions to promote a high degree of crystallinity in the process. In a general way sulfuric acid is the favorite chemical to isolate CNC due to its degradation potential for organic matter [24]. The yield to isolate CNCs depends on the raw material used, the type of acid, as well as the acid concentration, the ratio between biomass and acid (g/mL), temperature and the time. But according on literature review is possible to assured a general procedure. The acid hydrolysis of cellulose fibers will be carried on 65% (w/w) sulfuric acid. The temperature is a parameter that oscillate between room temperature to 70°C and for reaction time from 40 minutes to a few hours. After acid hydrolysis performance is necessary do other treatments to remove the excess acid content. To obtain CNC powder is essential go through a drying process [25].

4.5.1.1 Treatment with Phosphoric Acid

The acid hydrolysis treatment using phosphoric acid is of great interest because in addition to the introduction of phosphate groups instead sulphate (H_2SO_4 acid hydrolysis) groups when hydrolysis is realized causes changes in cellulose morphology form rod shape to spherical shape but only at certain conditions. The conditions to a successful phosphoric acid hydrolysis depends on the temperature. It is suggested that optimal temperature is at 100°C during two hours [26] But, according to [27] the optimal conditions are low temperatures and long reaction times and has the advantage that this treatment is a green method. As shown in **Figure 4-6** Based on literature, a determining factor is the way that is added the acid. Phosphoric acid need slowly added dropwise in solution temperature of below 20°C [28-29].
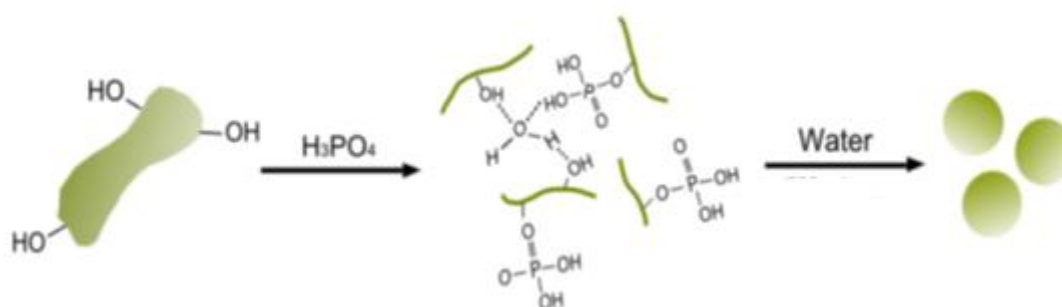
Figure 4-6. Dissolution of cellulose followed by it regeneration [27]

4.6   Characterization techniques

Characterization techniques are used to study the CNC that will allow us to know the morphology and structure of the material. The characterization techniques that we are going to cover in this thesis are Attenuated Total Reflection-Fourier Transform Infrared Spectroscopy (ATR-FTIR), X-Ray Powder Diffraction Spectroscopy (XRD), Stereomicroscopy, and Scanning Electron Microscopy (SEM).

4.6.1 ATR-FTIR Spectroscopy

Fourier Transform Infrared Spectroscopy is used in the characterization technique that allow us identify the functional groups present in the samples through the vibrational range of the infrared region (IR) (4000 cm^{-1} - 400 cm^{-1}). A trouble with this technique is does not allow to analyze samples directly in solid or liquid phase without any previous preparation. In some cases samples suffer from inevitable reproducibility issues given in the complexity of the sample preparation methods. When the molecules are excited to a higher state of energy absorbs Infrared radiation on order of 8 to 40 $kJ.mole^{-1}$. In the infrared range the bending and stretching vibrational frequencies of the bonds in the molecules are found. Since every molecule has a different vibrational frequency, the infrared spectrum can be used to indemnify molecules. To identify the chemical groups we need know that they vibrate at a specific frequency and be familiar with the frequencies at which absorb molecules (when they are excited to a higher state of energy). To obtain the individual absorption frequencies from the general complex signal called interferogram we need apply Fourier. It produces a spectrum virtually identical to that obtained with a dispersive spectrophotometer [30].

When the beam comes into contact with a sample the ATR use the property of total internal reflection and it measures the changes that occur in the totally internally reflected infrared beam. An infrared beam is directed into an optical crystal with a high refractive index (at certain angle) and this creates an evanescent wave that extends beyond the surface of the crystal into the sample held in contact with the crystal [30-31]. The working principle of ATR is shown in **Figure 4-7.**
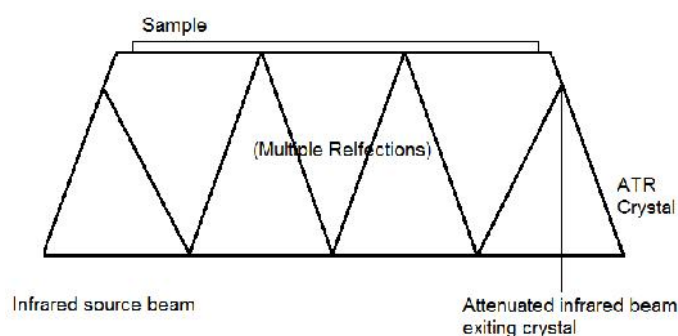
Figure 4-7. ATR working principle [32]

4.6.2 X-Ray Powder Diffraction Spectroscopy

The X-ray Disfraction (XRD) is technique which uses X-rays to quantify and investigate the crystalline nature of materials (regular sets of atoms). It is an experimental and non-destructive technique that allows us to know chemical composition, crystalline phases, shape, size, and internal stress of the material. X-rays are used because of their wavelength 10^{-10} m and nanometer 10^{-9} m region, since visible light has a length much greater than the space between atoms. The X-rays are produced when a particle electrically charged is rapidly decelerated. At the moment that the x-ray beam hits an electron, it produces the elastic scattering [33]. The waves interact with each other and occur two types of interferences. The most of them are canceling by destructive interference that cancels the waves, while a small percentage adds by constructive interference. This technique is based on constructive interference of X-rays. Satisfy Bragg's law ($n\lambda = 2d \sin \theta$) which relates the wavelength (λ) to the diffraction angle (θ), and the grating spacing in a crystalline sample (d) as shown in **Figure 4-8.** The diffraction peaks can be transformed to d-spacings allows identification of the materials. It is due each mineral has a set of unique d-spacings like a fingerprint. This technique bring us information about orientation distribution or interplanar distance of the planes depending on small changes in the manufacturing of the material [34].
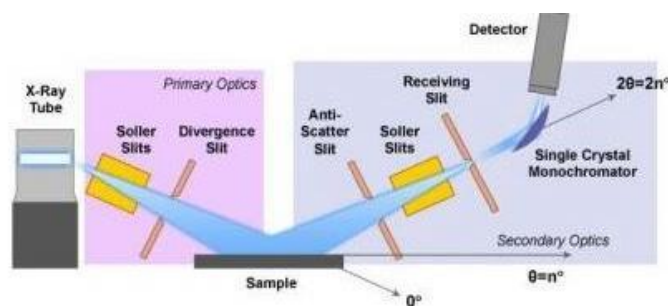
Figure 4-8. XRD working principle [33].

4.6.3 Stereomicroscopy

The Stereomicroscopy is a characterization technique that use an optical microscope allows observing the sample generating a three-dimensional image. In conventional microscopes, the sample is observed through a single objective, so this is the same for both eyes. While in the stereoscope the sample is observed through two different lenses, thus creating a three-dimensional effect as shown in **Figure 4-9**. This is because the image is slightly different and the brain interprets it as three-dimensional. This type of microscopes is light reflected by the sample is observed through the objectives and eyepieces. They are especially used for the analysis of unprepared samples. The magnification it has is less than the magnification of conventional optical microscopes. This is due to the optical aberrations induced by having two separate lenses. They generally have between 10 and 80x when combining the objectives and the eyepieces [35].

There are 2 main types of operating systems in these microscopes: Greenough and common main objective. In the Greenough microscope, the two objectives have a certain inclination between 10 and 12 degrees. This will create two slightly different images that provide a three-dimensional effect. In the common main objective microscope, the image is observed with a large objective, which projects a beam of light to each eyepiece. In this way, it is possible to generate a three-dimensional effect [35].
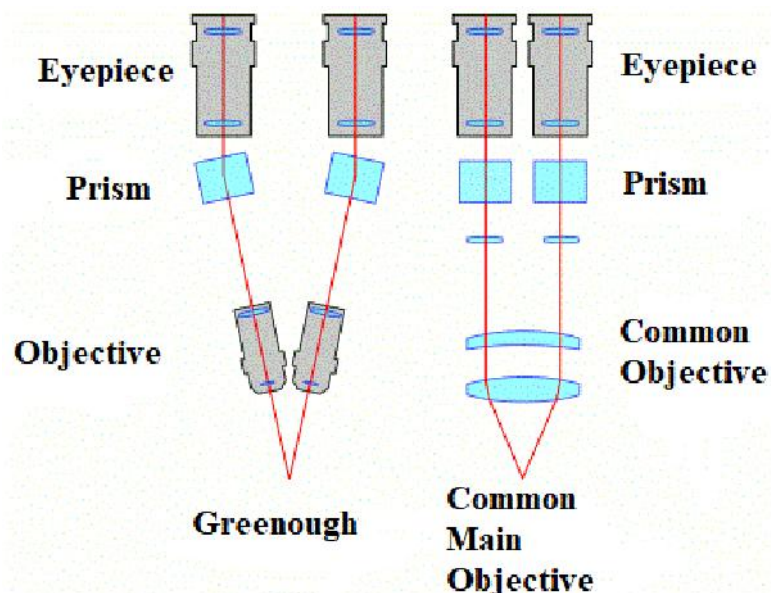
Figure 4-9. Stereomicroscope working principle [36]

4.6.4   Scanning Electron Microscopy

The scanning electron microscopy (SEM) is a characterization technique can provide information about crystal structure, topography, crystal orientation, phase distribution, electrical behavior, and chemical composition of some material. It is a high-resolution non-destructive microscope capable of images of the surface of a sample with a magnification can typically reach 10 - 500000 times and provides a detailed field with gray-scale images [37].   The principle of operation of this microscope consists on incident electrons beam, which is impacted on the surface of the specimen, and the reflected (or back-scattered) beam of electrons is collected. The energy that electrons lose (kinetic energy) when they "collide" with the sample can cause other electrons to fly off (secondary electrons), producing back-scattered electrons, X-rays, photons, heat, and visible light. Secondary electrons and back-scattered electrons are commonly used to image samples. Secondary electrons are used to show morphology and topography in the samples. The back-scattered electrons are used to illustrate compositional contrasts in samples [38] as shown in **Figure 4-10.**
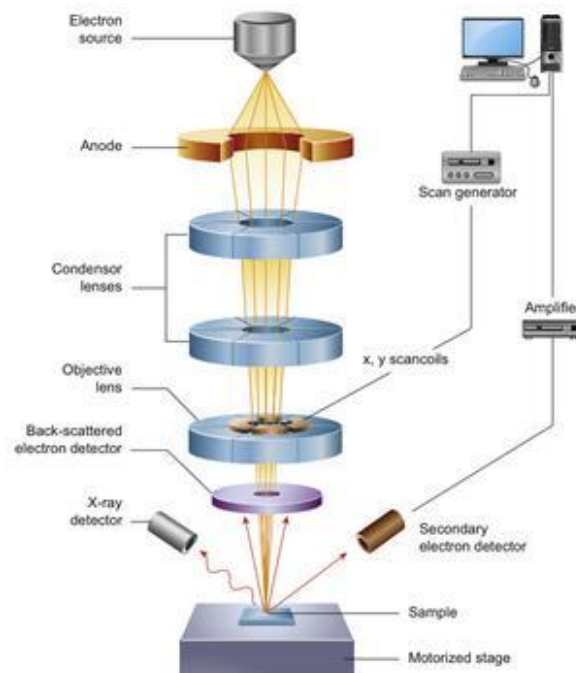
Figure 4-10. Schematic diagram of the core components of a SEM microscope [39]

4.6.5 Tensile Test

The tensile test has numerous purposes such as predict the performance of a material, guarantee quality, select a material for a determined application and so on. The two properties that are directly measured via a tensile test for our interest is the tensile strength and the maximum elongation. Tensile strength refers to is the stress required to break the sample. This measurement can be calculated by dividing the maximum load at breaking point by cross-sectional area and its units according to the International System is Pa. Maximum elongation is modulus of elasticity that is, the increase in length to the point of fracture comparing with the original length. This measurement is usually expressed as a percentage of the original length. From the previously explained measurements, there are some properties that can be calculated like Young's modulus and yield strength [40].

To realize this test is important mention that there is a standard tensile specimen that is shown in **Figure 4-11,** this ensures reproducibility of the method.
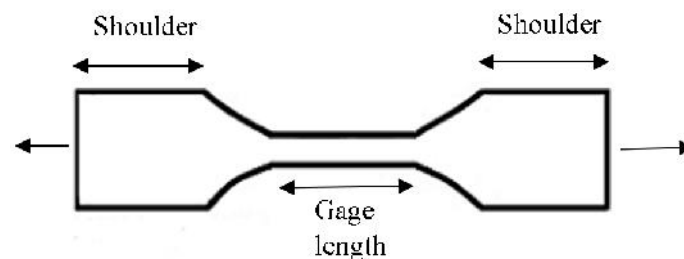
Figure 4-11. Standard tensile specimen

5   MATERIALS AND METHODS

5.1   Materials

Oil Palm Empty Fruit Bunch (OPEFB) was obtained locally, supplied by AgroPalma S.A. (Santo Domingo de los Tsáchilas, Ecuador), distilled water from Yachay Tech Laboratory, Sodium Hydroxide (NaOH) AR® (ACS) CAS: 1310-732, Glacial Acetic Acid (CH$_3$COOH) 99.99% EMSURE® 1000632500. Sodium Chlorite (NaClO$_2$) CAS:7758-19-2, Sulfuric acid (H$_2$SO$_4$, BAKER®ACS 97.99%,CAS:7664-93-9), Nitric acid (HNO$_3$) 65% EMSURE® 1004562500), Phosphoric acid (H$_3$PO$_4$, 85%, CAS: 7664-38-2), Commercial cellulose ((CC) average particle size of 50 μm) SIGMA-ALDRICH, CAS: 9004-34-6, Chitosan food grade (BioFitnest) (Guo Zhen international., LTD, viscosity 60-100 cps, >90% DD). About glass material used in the present work include: beakers (20000, 500, 250, 100, 50, 25 mL), Erlenmeyer flasks (2000, 250, 50 mL) volumetric flask (250, 50, 10 mL), Büchner funnel, filter paper (4-12 μm and 1-2 and 4 μm), glass watch, spatula, glass rod, hot plate, thermometers, magnetic stirrers, plastic containers, volumetric pipettes (10,5,2 mL), , graduated pipette (1 mL), micropipettes (0.1-1 mL and 0.5-5 mL), Pasteur pipette, universal support and clamps, wooden clamps, Innovating Science's (32mm x 20.4mm) dialysis tubing, Petri dishes (100mm x 15mm). The materials as well as reagents used during the development of this work were provided by the Yachay Tech Chemistry Laboratory.

5.2   Isolation of Cellulose Fiber

5.2.1   Fibers Pre-treatment

Cellulose was extracted from Oil Palm Empty Fruit Bunch. Previous to the extraction process, bunches required a pretreatment so, the OPEFB fibers were washed several times with distilled water to remove sugars and other water-soluble compounds as well as dust and any other physical impurities. The samples were dried at 40°C in the oven for 2 days until getting a constant weight. Once dried the palm biomass was cut to an approximate length of 5–10 mm.

5.2.2   Sodium Hydroxide Pre-treatment

To isolate cellulose is necessary a pre-treatment due to the cellulose is surrounded by hemicellulose and lignin, forming a lignocellulose matrix. The mechanism of alkaline pretreatment is the irreversible hydrolysis of the ester bond, weakening the structural integrity of the lignocellulose [41]. In the present work, the NaOH procedure was adapted from [42]. The OPEFB

fibers were treated with an alkali method with a 5% (w/v) NaOH solution. The conditions for the treatment were in a ratio of 1:20 g/ml, the temperature was constantly boiling at 80°C for 3h under magnetic stirring 500 rpm. As an important fact, after an hour a light layer of foam appear on the surface. Once the process finished, the fibers were washed with distilled water until to achieve 7 pH. And were dried overnight in the oven at 40°C before continuing the process.

5.2.3   Oxidation bleaching using NaOCl

The pre-treated fiber was bleached using Sodium Chlorite ($NaClO_2$) due to this reagent is a strong oxidant. For TCF bleaching, the work of [43] has been taken as a reference and has been adjusted for own purposes. The Oil Palm fibers were dissolved in distilled water in a ratio 1:32.5 g/ml. The solution was heated to 70°C. Once reached a constant temperature add 0.6 g of $NaClO_2$ and 0.4 ml of CH_3COOH per gram of pre-treated fiber. After an hour, the fiber has a brownish yellow color and it is necessary add the same amounts of $NaClO_2$ and CH_3COOH to acquire the optimal conditions of bleaching. The fibers were then boiled at 70°C for 2h under the magnetic stirring 500 rpm. The mixture was filtered with distilled water using a filter paper of 0.1 μm size pore. Then was dried in the oven at 40°C for 2 days.

To isolate cellulose from OPEFB were necessary three treatments. These process were adapted based on literature reported [44-45]. For a major comprehension, in **Figure 5-1** shows a general scheme of isolated OPEFB cellulose.
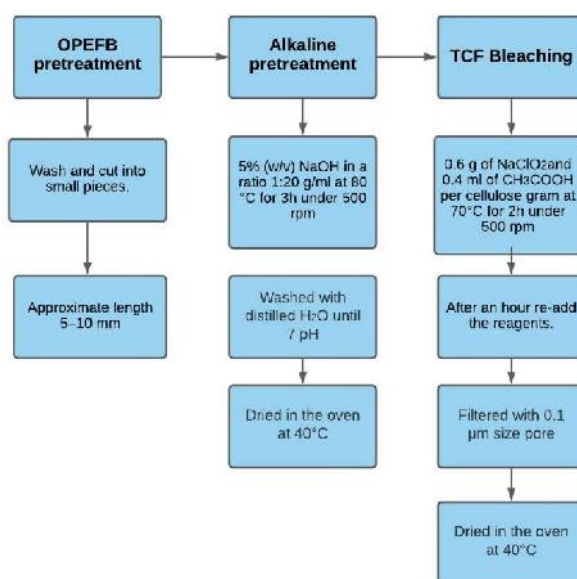
Figure 5-1. General scheme of isolation cellulose from OPEFB

5.3   Processing of CNC

5.3.1   Acid Hydrolysis

According with literature review, CNC isolation can be achieved with a chemical treatment [46]. Acid hydrolysis plays an important role for obtaining CNC due to separate of the amorphous cellulose. In order to evaluate the efficiency of acid hydrolysis in oil palm empty fruit bunch cellulose a micro-scale experiment was proposed using 65% H_3PO_4 at certain conditions. In this first trial, the influence of sonication before acid hydrolysis was studied.

5.3.2   Phosphoric Acid Hydrolysis

Phosphoric acid used in this reaction was diluted from (85% v/v) to (65% v/v). 1g of OPEFB cellulose were weigh and dissolved in 10 mL of distilled water. The dissolution was heated to 60°C. Simultaneously; 1 g of cellulose was sonicated for 5 min before heating process. Once two dissolutions reached a constant temperature of 60°, were slowly added 100mL of 65% H_3PO_4. The reaction time was 40 min under magnetic stirring 500 rpm. This mixture was subsequently cooled in an ice bath to room temperature. Once processes finished, the mixture were filtered with distilled water using a filter paper of 0.4 μm size pore and were dried overnight in the oven at 40°C. To optimize the phosphoric acid hydrolysis process is suggested   a set of experiments that facilitate evaluate and decide which the best methodology that we can choose is to isolate OPEFB CNC.

5.3.3   Optimization of Phosphoric Acid Hydrolysis

Different treatments for phosphoric acid hydrolysis were proposed in order to evaluate the efficiency to isolate CNC from OPEFB cellulose. The effectiveness of phosphoric acid hydrolysis on OPEFB cellulose were tested by changing reaction parameters. The parameters to evaluate it influence were acid concentration, ratio cellulose/acid, time and temperature. In total 14 experiments were carried out and for each experiment was used 0.5 g with a particle size of 120 MESH or less. All reactions had a constantly centrifugation stirring speed 700 rpm. Each sample had the same treatment but under different conditions that can be seen arranged in the **Table 5-1**. About sample naming of CNC samples is proposed based on reaction conditions of acid hydrolysis. For example: PA-45-3.5-70 for an input of OPEFB cellulose was hydrolyzed with 70% (v/v) phosphoric acid in a ratio 1:50 g/ml, at 45°C during 3.5 hours.

Table 5-1. Experiments of Phosphoric Acid Hydrolysis

N° Exp.	Sample	Starting Material Cellulose	H$_3$PO$_4$ acid used mL	Conc. (v/v)	Ratio (g/mL)	Time (h)	Temperature (°C)	Quenching
1	PA-5-2.5-70	OPEFB	25	70	1:100	2.5	5	H$_2$O
2	PA-5-3.5-70	OPEFB	50	70	1:100	3.5	5	H$_2$O
3	PA-5-24-70	OPEFB	50	70	1:100	24	5	H$_2$O
4	PA-5-3.5-70-D	OPEFB	50	70	1:100	3.5	5	DMSO
5	PA-5-1-75	OPEFB	50	75	1:100	1	5	H$_2$O
6	PA-5-2.5-75	OPEFB	50	75	1:100	2.5	5	H$_2$O
7	PA-5-3.5-75	OPEFB	50	75	1:100	3.5	5	H$_2$O
8	PA-23-1-70	OPEFB	50	70	1:100	1	23	H$_2$O
9	PA-23-2.5-70	OPEFB	50	70	1:100	2.5	23	H$_2$O
10	PA-23-3.5-70	OPEFB	50	70	1:100	3.5	23	H$_2$O
11	PA-23-24-70	OPEFB	35	70	1:70	24	23	H$_2$O
12	PA-45-3.5-70	OPEFB	25	70	1:50	3.5	45	H$_2$O
13	PA-63-1-70	OPEFB	25	70	1:50	1	63	H$_2$O

The sample labeled as blank refers to an unhydrolyzed cellulose sample in order to compare with modified OPEFB cellulose. According literature, in acid hydrolysis DMSO is a great reagent for quenching [47] but the purpose of this work is establish a green methodology that is why the hydrolysis reaction was quenched by adding 100 mL of cold distilled water (5°C) except for one sample that used 30 mL of tempered 25% DMSO. This was realized with the purpose of evaluating the effectiveness of distilled H$_2$O to precipitate the cellulosic material. After quenching process, all experiments were sonicated for 10 min followed by centrifugation. The conditions of the centrifugation step influences in the yield and the dimensions of CNCs [48]. The samples were placed in 50 mL centrifuge tubes and centrifuged at 10,000 rpm for 10 min. The suspension samples were submitted at two cycles of centrifugation that help to remove the excess acid for a posterior treatment.

5.3.4 Dialysis

This technique is necessary due to the importance of remove all acid content [49]. All samples were put on dialysis tubes (32mm x 20.4mm) as is shown in **Figure 5-2**. For each sample was performed dialysis against distilled water to remove free acid molecules from the suspensions. OPEFB cellulose samples were dialyzed for 5 days until to achieve neutral pH. The distilled water of each beaker was exchanged every day. After dialysis, all samples were sonicated for 5 min to disperse the nanofibers. The result of this process is important to collect the samples for subsequent characterization analysis.

Figure 5-2. Dialysis System to cellulose from OPEFB

5.3.5 Freeze-drying

Lyophilization is a process where a frozen sample is sited under a vacuum with the purpose of removing water. Its operating principle is sublimation; it means that H_2O content of sample change directly from solid to vapor [50]. A drying step is essential to achieve CNC powder from the aqueous suspension. All samples after dialysis process were freeze-frying in order to continue the research. CNC suspension were put on 25 mL centrifuge tubes and freeze at -80°C. The freeze dryer of biology department works at 200 Pa and -50°C as shown in **Figure 5-3**. An advantage of this process is the preservation of chemical structure and integrity of sample.

Figure 5-3. Freeze-drying process on CNC from OPEFB

To isolate Crystalline Nano-Cellulose from OPEFB were necessary different processes. The followed methodology is shown in **Figure 5-4**.
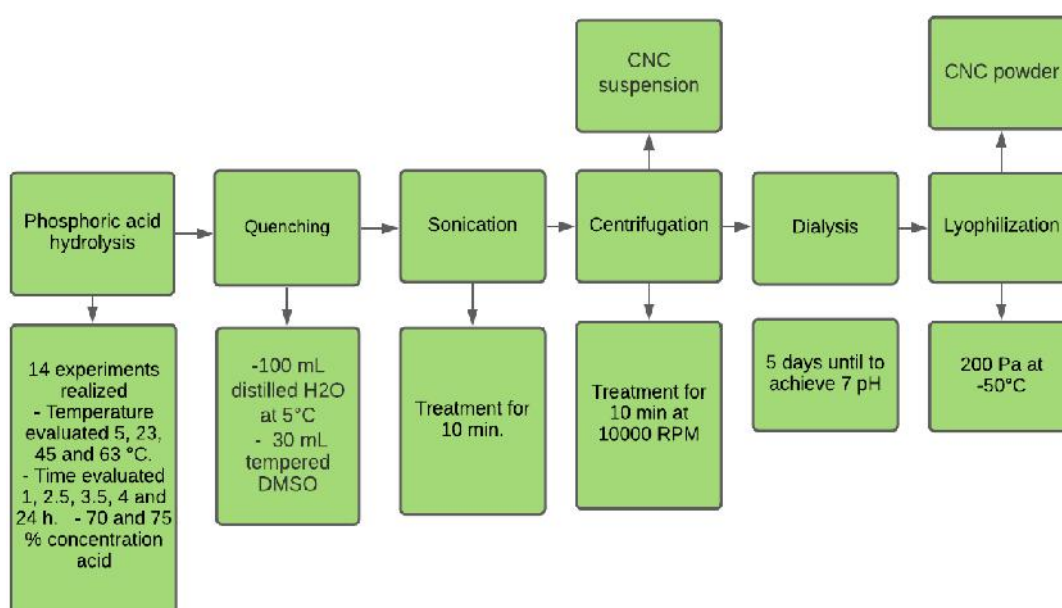
Figure 5-4. General scheme of isolation CNC from OPEFB

5.4   Chitosan/ CNC Film Preparation

All sample films were prepared by a casting method [51]. First, an aqueous solution of acetic acid 2% (450 mL) was prepared in a 500 mL beaker. Then, add chitosan 2% w/v to the solution for dissolving [52]. The conditions for the treatment were a ratio of 2:100 g/ml, the temperature was constantly at 40°C under magnetic stirring 800 rpm during 3 hours. After that, modified OPEFB cellulose 2% w/w was added while stirring, and the solution was mixed for at least 1 h. The

composition of the films chitosan – OPEFB cellulose on a dry basis is 50:50. An important step before add the cellulose is sonication. Each sample was sonicated for 15 mins at room temperature. The solutions (30 mL) were cast on Petri plastic dishes 100mm x 15mm for compression-molding to produce films of uniform width and place at room temperature overnight shown in **Figure 5-5**. The films were completely dried to the next morning and each film was unstick from it Petri dish and was stored on the same plates.
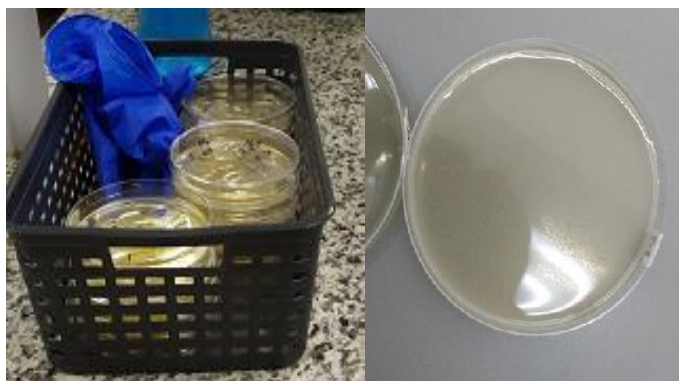
Figure 5-5. Films of chitosan/ modified OPEFB cellulose

5.5 Characterization Techniques

The characterization of the obtained materials provides comprehensive information about the structure and properties which are useful for many applications. The characterization techniques offer physicochemical and morphological study to describe the structure of modified OPEFB cellulose with phosphoric acid.

5.5.1 ATR-FTIR Spectroscopy

FTIR measurements of CNC samples were taken using Varian 670-IR Spectrometer, with 64 scans in the range from 400 to 4000 cm^{-1} and a resolution of 4 cm^{-1}. This technique was used with the purpose assign all critical bands to cellulose and discard the existence of lignin and hemicellulose content. Also it was possible calculate LOI that offers a qualitative view respect to crystallinity. In **Figure 5-6** is observed the sample analysis
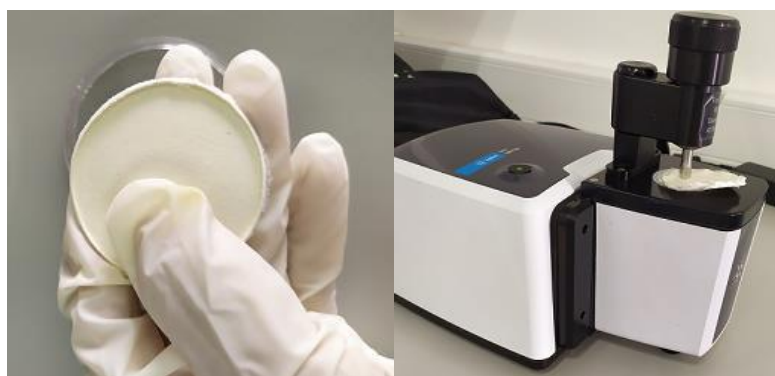
Figure 5-6. ATR-FTIR sample analysis

5.5.2   X-Ray Powder Diffraction Spectroscopy

For this work, CNC samples were dried until a flat film was obtained. Then, they were analyzed in a powder diffractometer Miniflex-600, Rigaku, with a D/tex Ultra2 detector as is shown in **Figure 5-7**. The X-ray generator was operated at 40 kV and 15 mA, in a sealed tube CuKa radiation source. The Xc was calculated for all modified OPEFB samples according Equation 1. from an internal reference method of Segal [53].

$$CI = \frac{I_{200} - I_{am}}{I_{200}} x100 \tag{1}$$

Where I_{200} is the intensity value for the crystalline cellulose ($2\theta = 22.5°$) and I_{am} is the intensity value for the amorphous cellulose ($2\theta = 18.5°$).

Figure 5-7. XRD sample analysis

5.5.3 Stereomicroscopy

A morphology study of a first stage of OPEFB cellulose hydrolyzed with phosphoric acid (sample withs sonication and no sonication) was carried out in SZX16 stereomicroscope (Olimpus). The sample preparation is shown in **Figure 5-8.**
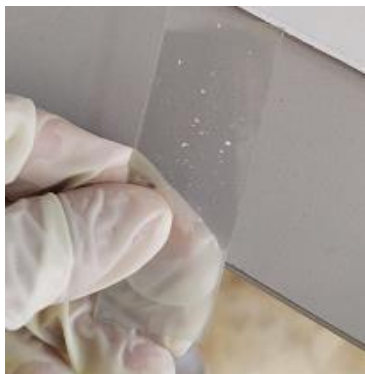
Figure 5-8. Prepared sample for Stereonicroscopy

5.5.4 Scanning Electron Microscopy

SEM images from all hydrolyzed samples were taken using a Phenom ProX Desktop SEM, where primary electron energy was 10 kV and a magnification of 1000x and 100000x. Prepared samples are presented in **Figure 5-9.**

Figure 5-9. Prepared samples for SEM

5.5.5   Tensile Test

Tensile strength testing was performed on UNITED SSTM "SMART" TABLE MODEL as shown in **Figure 5-10**. The loading speed was 5.0 N/ min. modulus of elasticity and tensile strength were determined for all samples. The thickness of samples was variable between 0.07 and 0.16 mm. For each chitosan/ modified OPEFB cellulose film samples were made five repetitions.
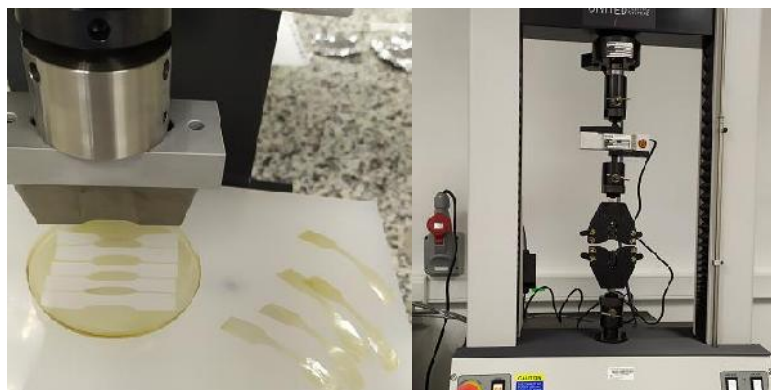
Figure 5-10. Tensile Test

6   RESULTS AND DISCUSSION

As previously described, OPEFB cellulose were isolated in order to obtain materials whose main purpose is to use as green filler. This study aims to characterize the isolated cellulose nanocrystal (CNC) from OPEFB in presence of phosphoric acid at certain conditions based on literature review to do an evaluation and propose a methodology. The next step in this work is the optimization of a process using the acid that best suits. 13 experiments were performed in phosphoric acid hydrolysis to evaluate the influence of temperature, acid concentration, ratio cellulose and acid, time on the effectiveness to produce CNC from OPEFB. Finally, for each material obtained its mechanical properties were evaluated with the purpose of ensure that they function as green fillers to chitosan films.

6.1   Isolation of Cellulose Fiber

The isolation process has three steps to achieve cellulose fiber from OPEFB. First a pretreatment to the raw material with the purpose of removing any physical impurities as well as water-soluble compounds like sugars. The next steps were necessary to eliminate hemicellulose, lignin and ashes content from OPEFB. Fisrt, a basic hydrolysis with NaOH where there is an observable result. Fiber change the brown-dark color to brown-yellowish fiber color. Then a TCF bleaching treatment where the fiber suffered a size decrement and turned white completely as shown in **Figure 6-1**.

Figure 6-1. Isolated cellulose from OPEFB

Once dried the OPEFB cellulose were ground to smaller particle size and then the solid was sieved using Stainless Steel Mesh Sieve Set. The different size obtained are shown in **Table 6-1**

Table 6-1. Cellulose particle size obtained from OPEFB

Particle size		Sample	Percentage
MESH	Micron (μm)	Weigh (g)	(%)
35	500	0.47	3.04
60	250	4.27	27.66
120	125	6.42	41.58
230	63	2.77	17.94
<230	<63	1.51	9.78
	TOTAL	15.44	100

The cellulose fiber yield produced from this proposed treatment was 51.5 % (w/w). This result is according with the literature review. The cellulose content from oil palm empty fruit bunch oscillates between 44 – 64 % in dependence of plant nature as well as the hydrolysis conditions [54-55]. The next step for this cellulose is its characterization, this will allow us to know its properties as well as evaluate the effectiveness of the method to o eliminate the hemicellulose and lignin content.

6.2   Isolation CNC from OPEFB

To evaluate the efficiency of conditions for a phosphoric acid hydrolysis were proposed 14 different treatments. The parameters that were changed to evaluate it influence were different ratio cellulose/acid as well as acid concentration, time and temperature. This study is fundamental for deciding the best methodology respect to phosphoric acid hydrolysis on OPEFB cellulose. In the **Table 6-2** can be seen arranged the results according to the temperature at which each experiment was carried out. This parameter was chosen as the one of greatest interest for what will be discussed below.

Table 6-2. Yield percentage after H3PO4 hydrolysis

Sample	H$_3$PO$_4$ acid		Initial Weigh (g)	Final Weigh (g)	Yield (%)
	used mL	Ratio (g/mL)			
PA-5-2.5-70	25	1:100	0.254	0.203	79.992
PA-5-3.5-70	50	1:100	0.502	0.399	79.594
PA-5-24-70	50	1:100	0.504	0.374	74.156
PA-5-3.5-70-D	50	1:100	0.504	0.361	71.531
PA-5-1-75	50	1:100	0.504	0.378	75.060
PA-5-2.5-75	50	1:100	0.503	0.390	77.512
PA-5-3.5-75	50	1:100	0.500	0.280	55.951
PA-23-1-70	50	1:100	0.503	0.406	80.740
PA-23-2.5-70	50	1:100	0.503	0.411	81.709
PA-23-3.5-70	50	1:100	0.500	0.410	81.510
PA-23-24-70	35	1:70	0.502	0.214	42.703
PA-45-3.5-70	25	1:50	0.502	0.245	48.825
PA-63-1-70	25	1:50	0.503	0.167	33.154

Based only on %yield data, is possible to ensure that exist a relationship between the temperature and the total yield of modified OPEFB cellulose. At 5°C samples PA-5-2.5-70, PA-5-3.5-70, PA-5-24-70 there is a slightly variation on yield (less than 6%) despite that the reaction time change from 2.5h until 24h. The acid concentration influences at acid hydrolysis because despite using low temperatures, it can be seen that at a time of 3.5h the yield of the sample drops by 28%. The major yield respect all samples were achieved at 23°C. Sample PA-23-24-70 was the exception and can be explained by the time of acid hydrolysis (24h). The decrement in yield is approximately of 50% compared to samples at the same temperature. The %yield for high temperatures (samples PA-45-3.5-70 and PA-63-1-70) cellulose change color drastically and decomposed that is why that no more tests were done to high temperatures. In **Figure 6-2** is more intuitive see the tendencies respect to the yield of phosphoric acid hydrolysis. The sample PA-5.3.5-70-D was not plotted cause quenching reagent is different than the other samples.
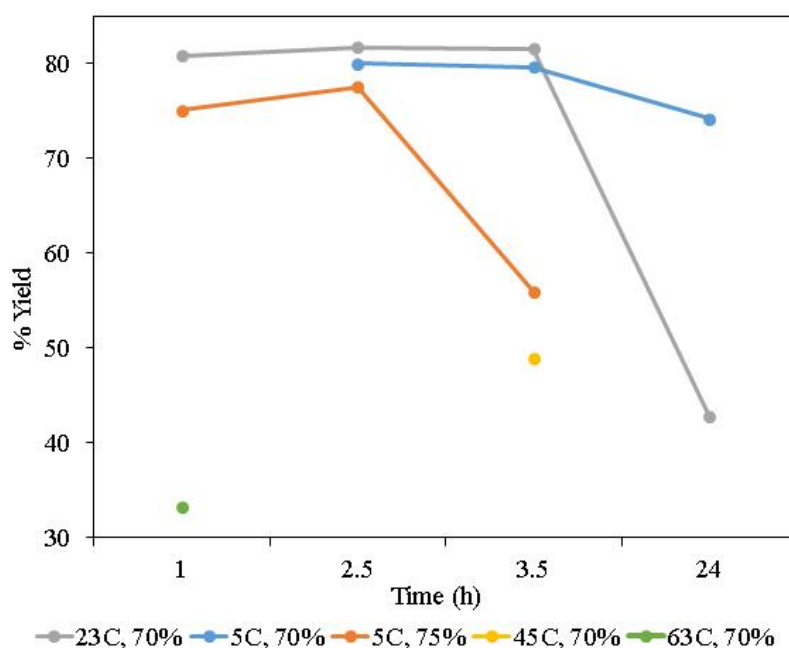
Figure 6-2Tendencies for samples after H3PO4 hydrolysis

The previous results offer us a perspective taking into account only the total yield of the reaction, but to evaluate the effectiveness of H_3PO_4 hydrolysis is essential to characterize each sample obtained. Is important to know them properties, chemical characteristics, % crystalline index, morphology, among others. The optimal procedure only can be determined after perform all characterization techniques for each sample. For a completely view of the process until the characterization of samples see **Annex1**.

6.3   ATR-FTIR Analysis

All spectra were subject to ATR correction, smoothing, baseline correction and being normalized. The present work uses the ATR- FTIR characterization technique to validate the nature of the sample (cellulose and CNC isolated form OPEFB) by assign characteristic signals corresponding to functional groups of pure cellulose and showing the absence of certain peaks that correspond to lignin and hemicellulose. The ATR- FTIR of the 14 modified OPEFB cellulose samples were realized but only three spectrums are shown. The reason is that the peaks assignation was similar in all samples and there are not found a significant difference. Based on literature there is a slightly differences in cellulose samples depends on which polymorph type is present.

All information about assignment of the signals were shown in **Table 6-3**. The spectrums shown in **Figure 6-3**, corresponding to samples PA-23-24-70, PA-5-24-70 and PA-5-2.5-70 which present cellulose polymorph type I, type II and a mixture of polymorph I and II respectively. For samples modified crystalline cellulose, the broad spectrum from 3700 to 3000 cm^{-1} contains –OH stretching vibration This band is observable as broad band for all presented samples but for sample PA-23-24-70 this band is medium broad. In the case of this sample that know belongs to cellulose polymorph type I. According to the literature, is possible determine if is cellulose Iα or Iβ for intermolecular hydrogen bond. It is expecting a signal at 3240 in the case Iα of or 3278 cm^{-1} for Iβ. In the spectra the signal is localized at 3240 cm^{-1}. For sample PA-5-2.5-70 that has cellulose polymorphs type I and II cannot be this band assign. Observables peaks in a range 2850-3000 cm^{-1} could be attributable to the symmetric and anti-symmetric stretching vibration modes in methylene groups (-CH$_2$). For samples PA-23-24-70 and PA-5-24-70 had one signal band at 2870 cm^{-1} while sample PA-5-2.5-70 had two signals in this region at 2910 and 2850 cm^{-1} [56-58].

The band at 1640 cm^{-1} correspond to bending vibration of absorbed water. This signal is present in all samples of modified crystalline cellulose of this work. The sharp peak at 1430 cm^{-1} is related to -CH$_2$ asymmetric bending (scissoring). In cellulose I, has a strong intensity than can be correlated with crystallinity. For cellulose type II and amorphous cellulose, the same peak could be shift slightly until 1420 cm^{-1}. For samples PA-23-24-70 and PA-5-2.5-70 is possible appreciate the band at 1430 cm^{-1} and the intensity between them, suggest that the first sample present higher crystallinity. Respect to sample PA-5-24-70 which belongs to cellulose type II, the same band has a faint displacement and it is observed at 1429 cm^{-1}. The peak at 1375 cm-1 is involved to C-H bending and peak 1318 cm-1 belong to CH$_2$ bending. Peaks at 1163 and 1112 cm-1 are related to stretch vibration of C–O–C and CH. The C–O–C skeletal vibration of polysaccharides ring is seen at 1034 cm-1. The peak at 896 cm-1 attributed to β-glycosidic linkages between the sugar units in cellulose. These signals are present of all modified OPEFB cellulose samples [56,59].

According with the ATR-FTIR spectrums of samples obtained showed no lignin presence. This can be clarified by the absence of the peaks at 1595, 1505, 1268 and 834 cm-1 that correspond to the aromatic skeletal vibrations of lignin. Respect to hemicellulose is more complicated to discard the it presence due to some bands are similar with cellulose so overlapped, but there is a peak at 1730cm-1 which correspond to stretch vibration of C=O acetoxy ester band is main associated

with hemicellulose content [56,60]. Only the sample PA-5-2.5-70 show this peak. Based on the ATR-FTIR results, it could be concluded that the chemical pretreatments and phosphoric acid hydrolysis were effective methods to remove lignin, hemicellulose, and wax of the fibers. In order to choose the best reaction conditions for phosphoric acid hydrolysis are necessary other characterization techniques.

Table 6-3. FT-IR assignments for samples

Wavenumber (cm-1)	Vibration type	Band assignments
3750–3000	ν O-H	Hydroxyl groups in lignin, cellulose and hemicelluloses Intermolecular hydrogen-bonded H–O–H stretching
3278		Iβ O6 H6···O3 intermolecular hydrogen bond
3240		Iα O6 H6···O3 intermolecular hydrogen bond
3000–2850	ν -CH2	Vibrational assimetric and symmetric CH2 in methylene
1732	ν C=O	Ester in acetoxy groups in hemicelluloses
1640	δ O-H	Adsorbed water
1595, 1505	ν C=Car	Aromatic skeletal vibration in phenolic ring of lignin
1430	δCH2	Asymmetric bending (scissoring)
1375	δC-H	C-H bending in cellulose
1318	δCH2	CH2 bending in cellulose
1268	νCar-O	νCar-O aromatic methoxyl group in lignin
1163	ν C–O–C	C–O–C asymmetric stretch vibration in cellulose
1112	ν C-H	CH stretching vibrations in different groups of cellulose
1034	νC–O–C	skeletal vibration of polysaccharides ring
896	νC1-O-C	β-(1–4)-glycosidic linkage
834		Oop bending of 1,2,4-tetrasubstituted aromatic in lignin
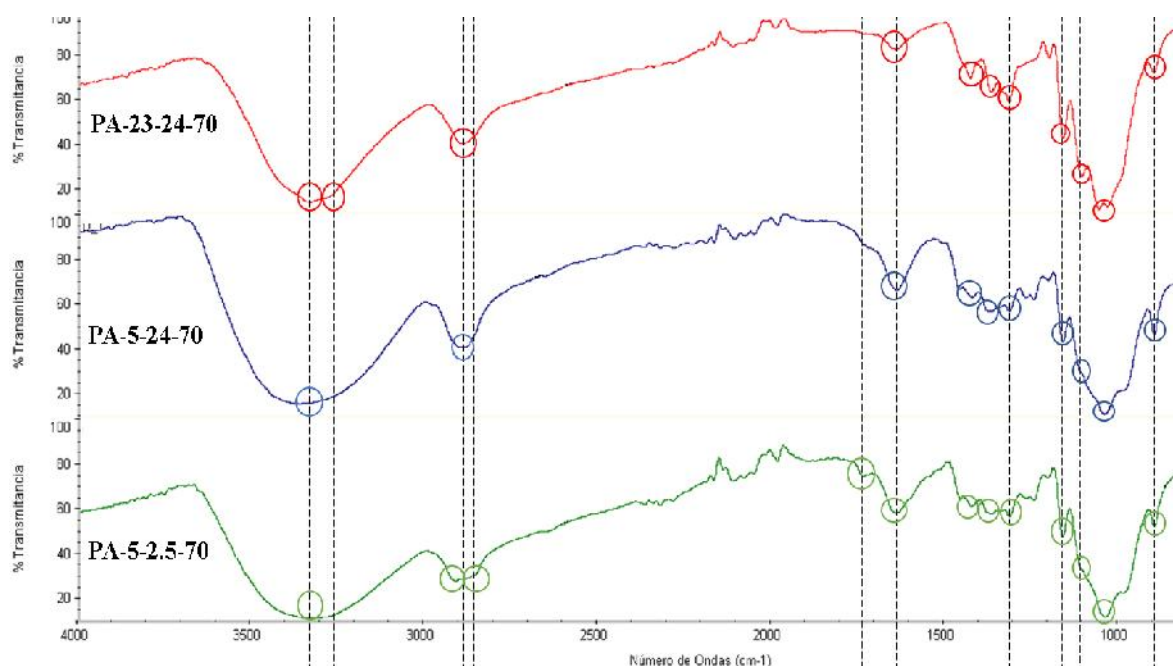
Figure 6-3. Main AFT-FTIR band in cellulose from OPEFB

ATR- FTIR technique also allows a study about the crystallinity of the material. In cellulose spectra there is two important peaks the first at 1430 cm^{-1} that correspond to the crystalline band of cellulose, and the second peak at 896 cm-1 that is attributed to the amorphous band of cellulose according with [61]. This is how the idea of Lateral Order Index (LOI) appears and it is defined as the absorbance ratio of A_{1430} to A_{896} [62]. So, LOI was calculated from selected areas to integrate and based on that deconvolution results were obtained. In **Figure 6-4** show the areas choose of sample PA-5-3.5-75 as sample. The rest of samples followed the same process. LOI results are shown in **Table 6-4**.
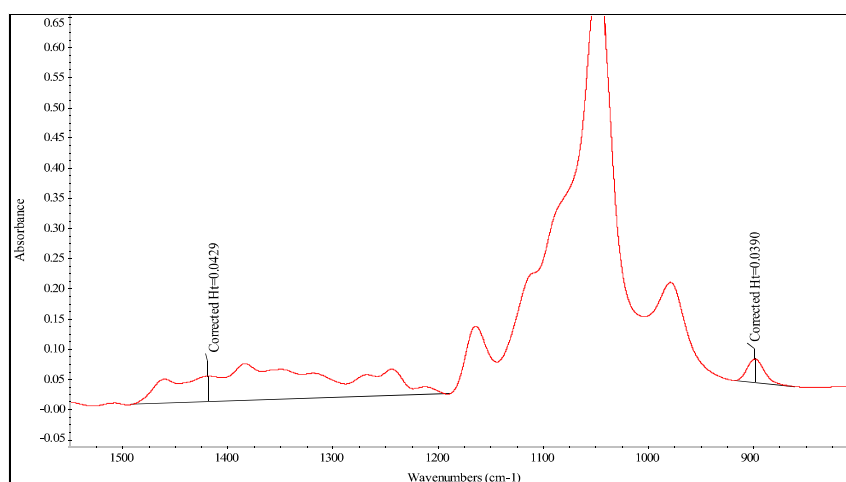
Figure 6-4. LOI calculation from ATR-FTIR spectra

Table 6-4. LOI results for modified OPEFB cellulose

Sample	LOI
Blank	1.66
PA-5-2.5-70	1.4
PA-5-3.5-70	2.11
PA-5-24-70	1.25
PA-5-3.5-70-D	2.43
PA-5-1-75	1.49
PA-5-2.5-75	1.69
PA-5-3.5-75	1.61
PA-23-1-70	2.11
PA-23-2.5-70	2.43
PA-23-3.5-70	1.11
PA-23-24-70	2.42
PA-45-3.5-70	2.43
PA-63-1-70	2.72

The sample label as blank belong to unhydrolyzed cellulose. The LOI allows us to have a qualitative idea about the crystallinity of materials. Then, LOI data will be compared with Xc calculated from XRD analysis at **Table 6-4**. To observe if there is a correlation between characterization techniques from crystalline materials.

6.4   XRD Analysis

X-ray diffraction technique were used to study the crystallinity behaviors of cellulose treated with different conditions of phosphoric acid hydrolysis. The obtained results are presented according to the temperature at which each experiment was carried out. This is due to on section 4.2 the temperature was a significant parameter. With this characterization technique it pretends that make a correlation between temperature and % crystalline index if it is possible. All the diffractograms presented below were normalized and the applied XRD range was from 5° to 50° 2θ due to the relevant band intensities are in this region. The analysis covers the crystalline and amorphous cellulose components that let us know important information for assign the cellulose polymorphs

present in each sample Also is calculated the % crystalline index for each sample. The crystallinity index of the samples was calculated according to **Equation 1**.

6.4.1 Sample as reference

The sample blank belong to unhydrolized cellulose; this sample was carried out with the purpose of taking a reference point respect to acid hydrolysis. The diffractogram shown in **Figure 6-5**, exhibits three crystalline peaks, the 2θ equal to 14.38°, 15.93° and 22.17° and 34.81° which are assignable to the planes ($1\bar{1}0$), (110), (200) and (040) respectively. These values were assigned in agreement with the diffractogram patterns reported in [63,64] that correspond to cellulose I polymorph. For an indicator of crystallinity for the sample, CI % was calculated and in the sample B is 79.1%. This means that exist high alignment between its chains and we have a crystalline material.
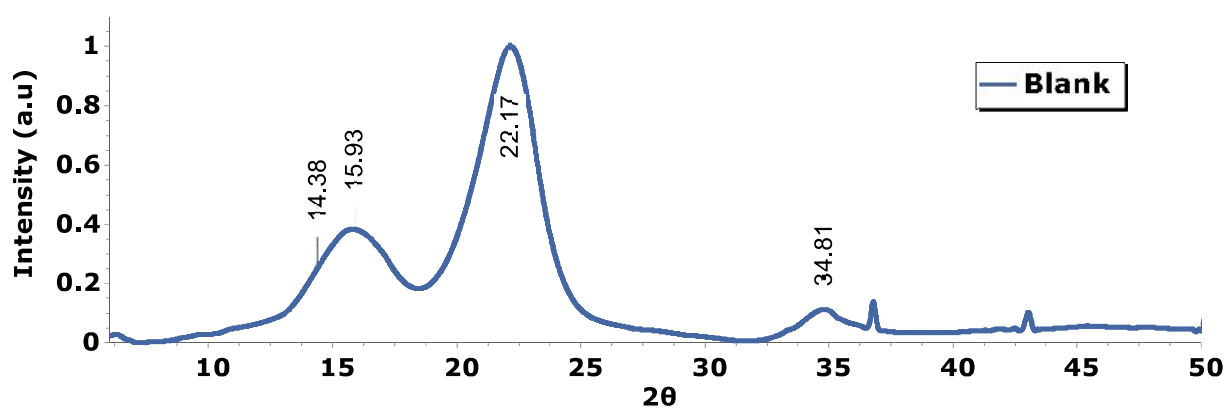
Figure 6-5. XRD diffractogram – Unhydrolized cellulose

6.4.2 Samples at low temperature

According with **Table 6-2** there are 8 experiments realized at 5°C but the temperature is the only conditions that is equal for this set samples. So, the samples that used 70% (v/v) phosphoric acid for the acid hydrolysis will be analyzed first. Then, will be discussed the samples where acid hydrolysis was performed at 75% (v/v) phosphoric acid.

6.4.2.1 Samples at 70% (v/v) phosphoric acid

For this set samples notice that the diffractograms of sample PA-5-2.5-70 and PA-5-3.5-70 are slightly related. The experimental procedure for this OPEFB cellulose samples were similar except for the time reaction and the ratio cellulose and acid. The XRD patterns shown in **Figure 6-7** were difficult to relate to one cellulose polymorph, which is why the presence of more than one type of cellulose arises. For cellulose I polymorph, it expected four major crystalline peaks which belong to the planes $(1\bar{1}0)$, (110), (200) and (040) at $14.8°$, $16.3°$, $22.6°$ and $34.5°$ in 2θ axis. For sample PA-5-2.5-70 the peaks were identify at $14.76°$, $16.28°$, $22.28°$ and $33.31°$ and in the case of sample PA-5-3.5-70 the corresponding peaks were $14.87°$, $16.35°$, $22.24°$ and $34.23°$ in 2θ axis. For cellulose II polymorph, it expected three peaks: $12.1°$, $19.8°$ and $22°$ at 2θ axis which belong to the planes $(1\bar{1}0)$, (110) and (200) respectively. In sample PA-5-2.5-70 was possible to detect the peaks at $11.05°$, $19.15°$ and $22.28°$ and for sample PA-5-3.5-70 these peak $11.06°$, $19.13°$ and 22.24 were allocated [63-65]. The obtained peaks have a short displacement comparing with the literature peaks but all values can be correctly allotted. The observable peak for (200) plane is equal to both polymorphs cause the peak is overlapped. For the amorphous region related to $\approx 18.5°$, is possible to notice a single broad peak more sharpness in sample PA-5-3.5-70 than sample PA-5-2.5-70, which indicates that sample PA-5-3.5-70 will have higher Xc than sample PA-5-2.5-70. The calculated Xc is 41.6% for sample PA-5-2.5-70 and 75.35% for sample PA-5-3.5-70. This results support the idea of the ratio cellulose and phosphoric acid during acid hydrolysis is a determining factor.

Figure 6-7. XRD diffractogram – Sample PA-5-2.5-70 and PA-5-3.5-70

For sample PA-5-24-70, the diffractogram shown in **Figure 6-6**, is too different to those shown in the samples PA-5-2.5-70 and PA-5-3.5-70 despite sharing reaction conditions. The XRD pattern display three crystalline peaks, the 2θ equal to 11.1°, 19.59° and 22.22° which are assignable to the planes $(1\bar{1}0)$, (110) and (200) respectively. In correspondence with the literature this diffractogram belong to cellulose II polymorph. The calculated Xc is 53.3%. In this sample the time was a determining factor all cellulose I polymorph were transformed into cellulose II polymorph so, the crystalline index will be affected.
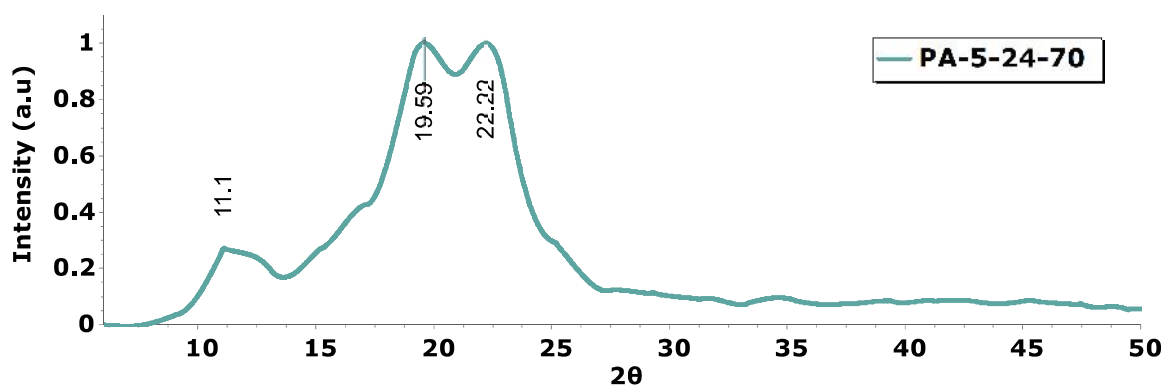
Figure 6-6. XRD diffractogram – Sample PA-5-24-70

The sample PA-5-3.5-70-D was carried out with the purpose of evaluating the quenching way. This experiment was precipitated using tempered DMSO instead cooled distilled water like the rest of experiments. Its XRD pattern shown in **Figure 6-8**, exhibit four crystalline peaks at 2θ equal to 14.66°, 15.97°, 21.75° and 33.89° which are assignable to the planes $(1\bar{1}0)$, (110), (200) and (040) respectively. The present polymorph is cellulose type I and Xc is 80.7. The sample PA-5-3.5-70 (CI equal to 75.35%) have the same reaction conditions so is possible affirm that the use of DMSO increments the crystallinity of the sample.
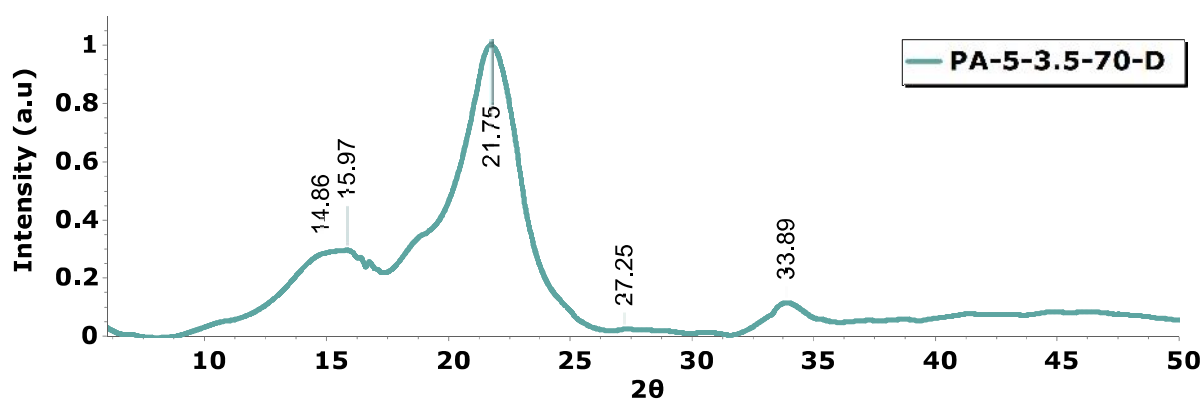
Figure 6-8. XRD diffractogram – Sample PA-5-3.5-70-D

6.4.2.2 Samples at 75% (v/v) phosphoric acid

In this set samples, the diffractograms of samples PA-5-1-75 and PA-5-2.5-75 are similar. The XRD patterns shown in **Figure 6-9**: were similar to samples PA-5-2.5-70-D and PA-5-3.5-70 so, a similar analysis is proposed. For cellulose I polymorph, it expected four major crystalline peaks which belong to the planes $(1\bar{1}0)$, (110), (200) and (040) at 15.11°, 17.12° , 22.39° and ≈34.5° that is not appreciated for sample PA-5-1-75 diffractogram. The peaks for sample PA-5-2.5-75 were at 14.81°, 16.38°, 22.18° and 34.64° in 2θ axis. In the case of cellulose polymorph type II have three significant peaks, for sample PA-5-1-75 were at 11.06°, 19.45° and 22.39° which are assignable to the planes $(1\bar{1}0)$, (110) and (200). In sample PA-5-2.5-75 was possible to detect the peaks at 12.57°, 19.55° and 22.18°. The observable peak for (200) plane is equal in both polymorphs because they are overlap. Based on XRD fitting the calculated Xc is 42.2% for sample PA-5-1-75 and 60.8% for sample PA-5-2.5-75. In this case, the time of acid hydrolysis is a determining factor. If the reaction time is very short, the acid hydrolysis is deficient, so we will have lower Xc.
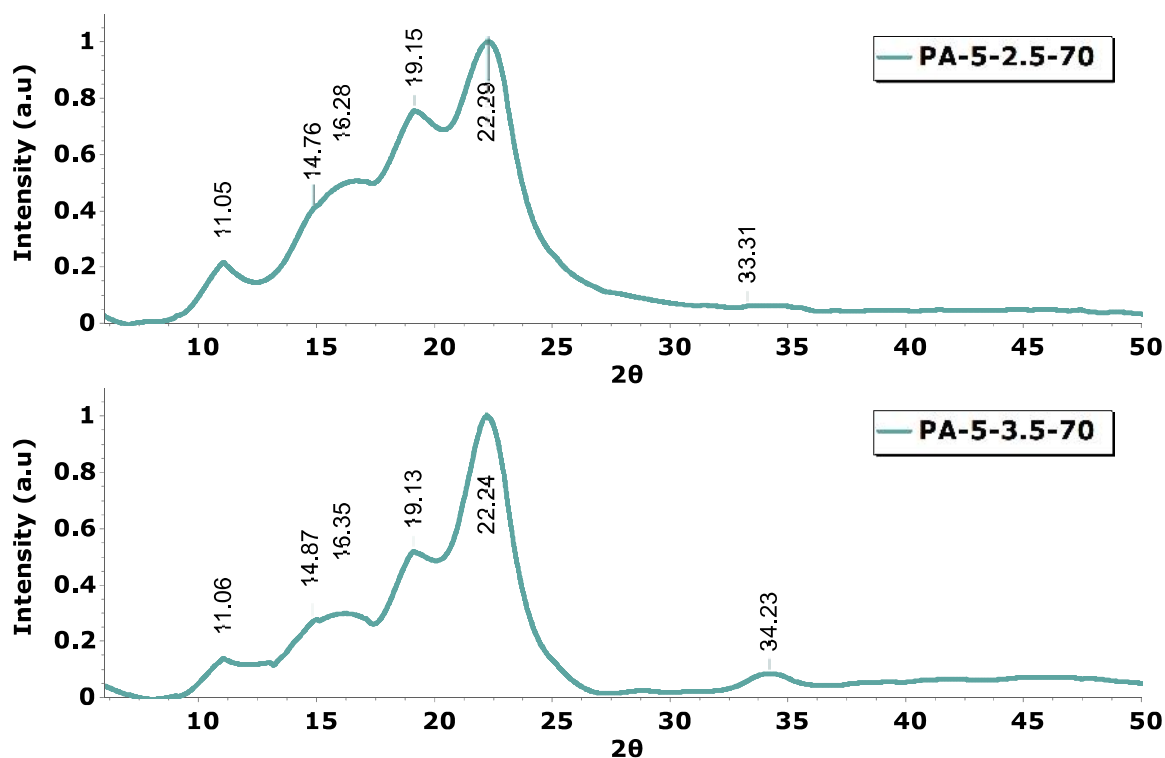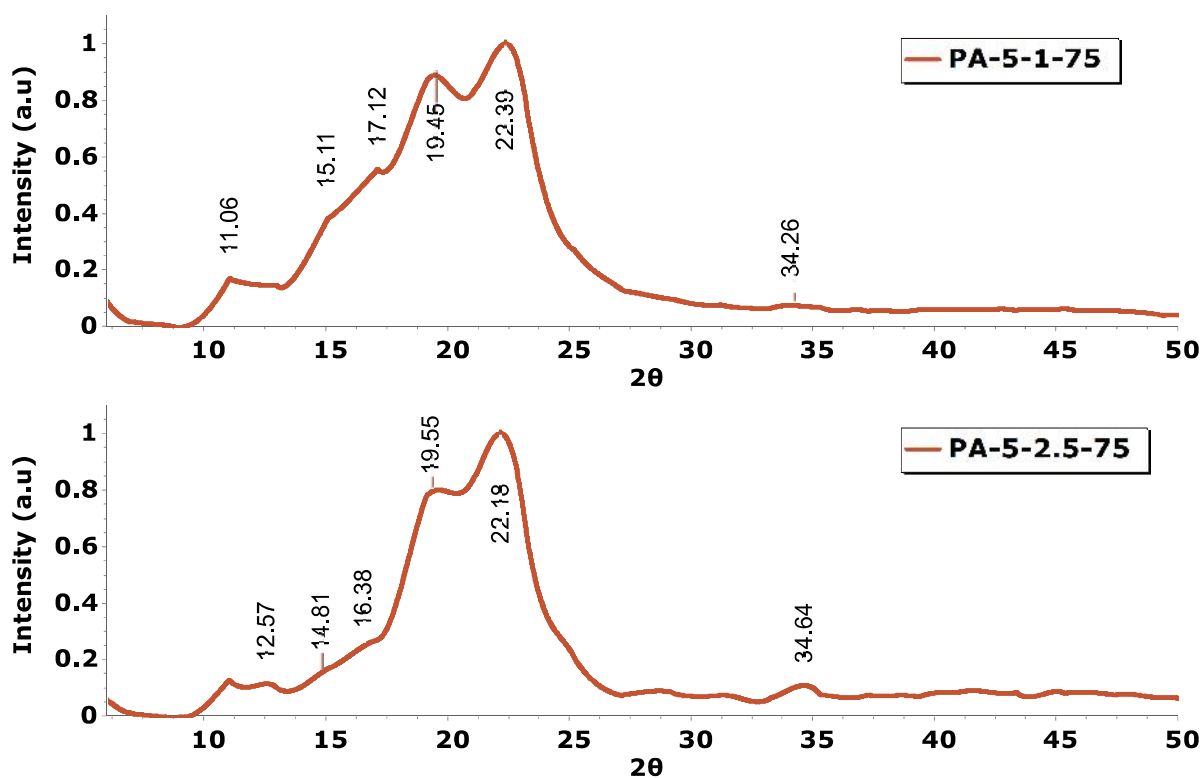
Figure 6-9. XRD diffractogram – Sample PA-5-1-75 and PA-5-2.5-75

For sample PA-5-3.5-75, the diffractogram shown in **Figure 6-10**, is slightly different to previous samples despite sharing reaction conditions. Based on presence of two polymorphs is possible to identify four crystalline peaks for cellulose I, the 2θ equal to 13.08°, 16.3°, 22.31° and 35.27° which are assignable to the planes (1$\bar{1}$0), (110), (200) and (040) respectively. For cellulose type II have three peaks, 11.94°, 20.13° and 22.31° which are assignable to the planes (1$\bar{1}$0), (110) and (200). The observable peak for (200) plane is equal in both polymorphs because they are overlap. The calculated Xc is 61.7%. The slightly increment on crystallinity is observed due to this sample had a reaction time bigger that other samples at the same conditions.
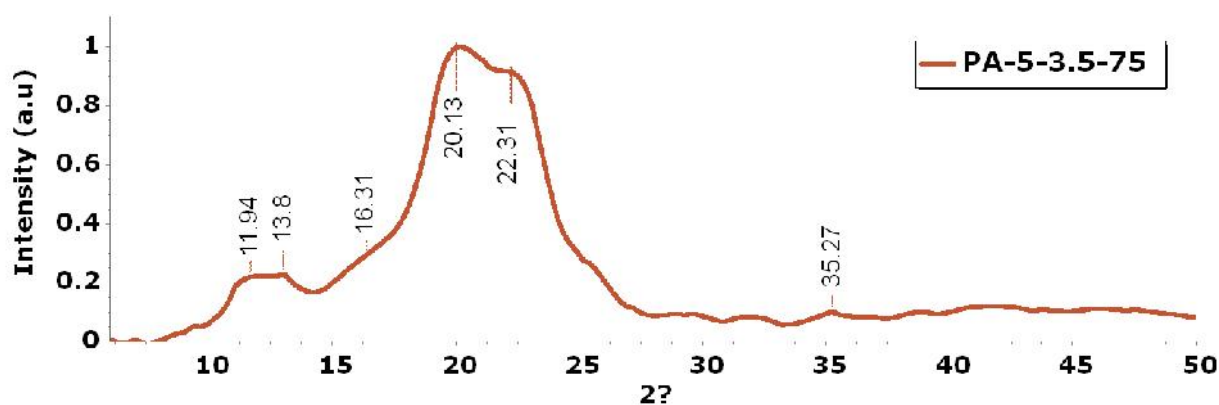
Figure 6-10. XRD diffractogram – Sample PA-5-3.5-75

6.4.3 Samples at room temperature

According with **Table 6-2** there are a set of 4 samples PA-23-1-70, PA-23-2.5-70, PA-23-3.5-70 and PA-23-24-70. The diffractograms of all them are similar as are shown in **Figure 6-11**. For cellulose polymorph type I the peaks related with planes ($1\bar{1}0$), (110), (200) and (040) were identify 14.89°, 16.16°, 22.53° and 34.63° for sample PA-23-1-70, peaks at 14.31°, 15.71°, 21.68° and 33.89° for sample PA-23-2.5-70, peaks at 14.81°, 15.89°, 21.86° and 34.16° for sample PA-23-3.5-70 and 14.79°, 15.85°, 21.59° and 33.71° for sample PA-23-24-70 in 2θ axis. For cellulose polymorph type II have three crystalline peaks at 12.73°, 19.16° and 22.53° for sample PA-23-1-70 and peaks at 11.03°, 19.06° and 21.86° for sample PA-23-3.5-70 which are assignable to the planes ($1\bar{1}0$), (110) and (200). Based on the projection peaks is possible assign the sample PA-23-1-70 and PA-23-3.5-70 with the presence of both polymorphs (cellulose type I and II). Respect to sample PA-23-2.5-70 there is only cellulose polymorph type I. The calculated Xc is 75.1.3%, 77.82%, 77.45% and 85.4% for sample PA-23-1-70, PA-23-2.5-70, PA-23-3.5-70 and PA-23-24-70 respectively. In this set samples despite time was different results that there is not a significant variation respect to crystalline index. So, these results support that is possible obtain high crystallinity percentage in user friendly conditions (acid hydrolysis 1:100g/ml at 70% H3PO4 at RT during 24 hours or less).
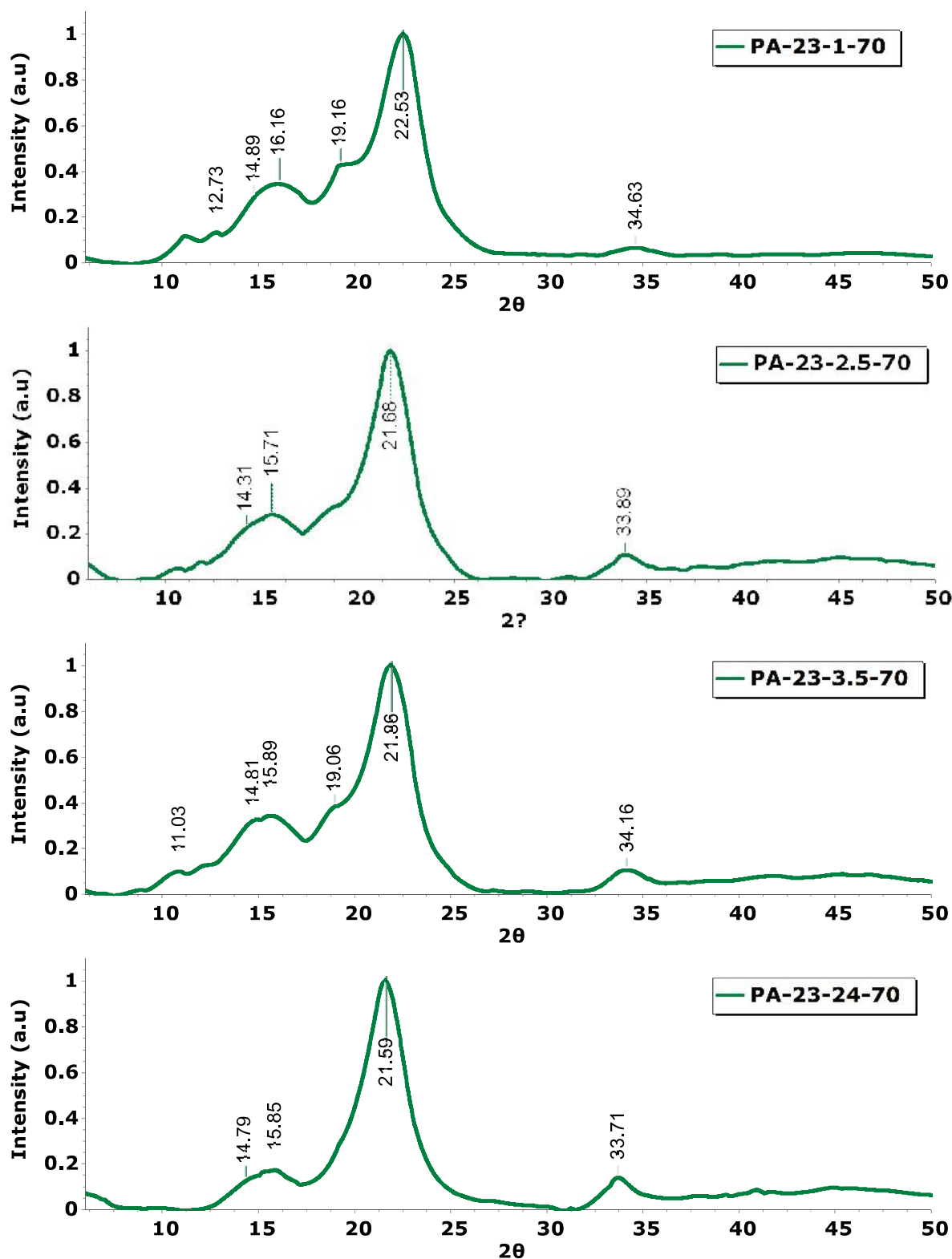
Figure 6-11. XRD diffractogram – Samples PA-23-1-70 PA-23-2.5-70, PA-23-3.5-70 and PA-23-24-70

.

6.4.4 Samples at high temperatures

According with **Table 6-2** two experiments were carried out at high temperatures. Due to the fact that during acid hydrolysis the cellulose changed from white to a cream color.

The XRD patterns of samples PA-45-3.5-70 and PA-63-1-70 are showed in **Figure 6-12**. The sample PA-45-3.5-70 analysis displays four crystalline peaks, the 2θ equal to 14.81°, 15.76°, 22.2° and 34.61° and for sample PA-63-1-70 show peaks at 14.99º, 16.78º, 22.48º and 34.76º which are assignable to the planes ($1\bar{1}0$), (110), (200) and (040) respectively. The values obtained in the samples show a slight displacement, despite these values can be assigned in agreement with to the literature reported that correspond to cellulose I polymorph. Based on XRD fitting the calculated Xc is 78.4% for PA-45-3.5-70 and 52.5% for PA-63-1-70. In the case of acid hydrolysis at high temperatures, the time and temperature are determining factors. At high temperatures the cellulose fibers decomposed by the acid so the time cannot be too long.
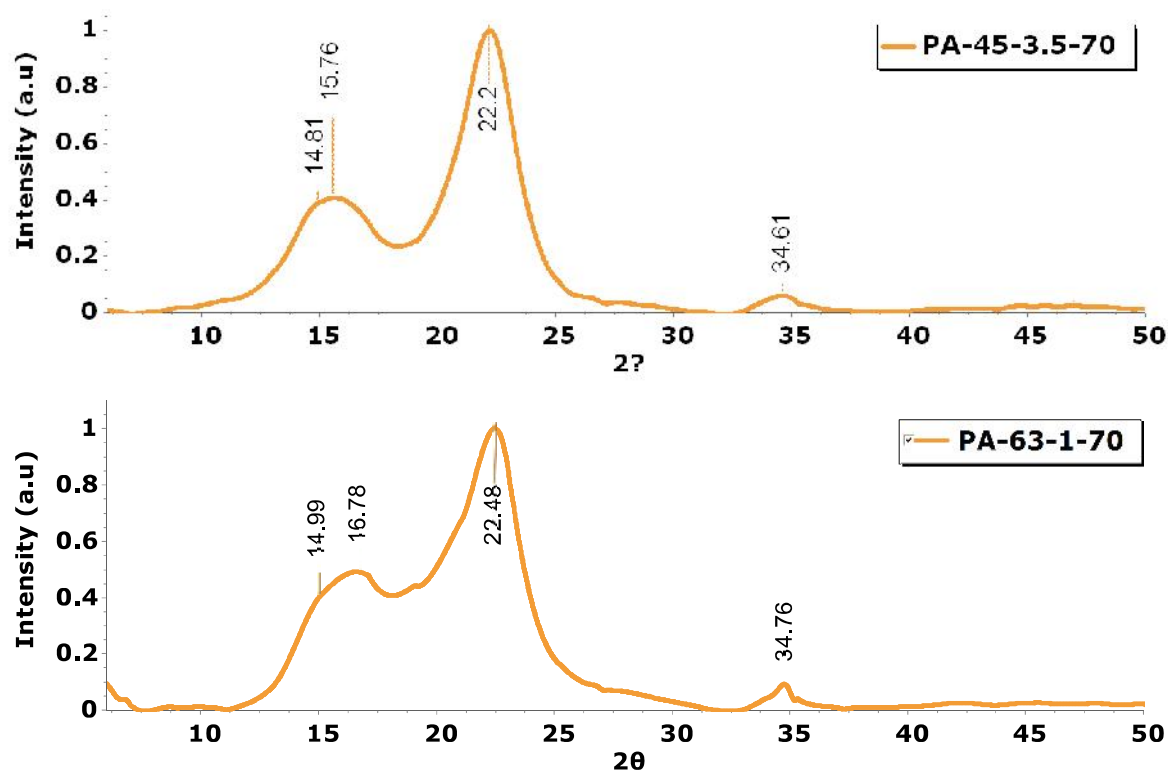
Figure 6-12. XRD diffractogram – Sample PA-45-3.5-70 and PA-63-1-70

For a major comprehension of XRD results were organized according to Xc also the most relevant found peaks of all XRD diffractograms are shown in **Table 6-5**: In a general way is possible affirm

that noteworthy peak changes represent the formation of the amorphous structure after acid hydrolysis. The changes in peak intensities, shapes and shifts denote changes of the crystalline structures in modified OPEFB cellulose [66].

Table 6-5. Summarize results of XRD technique for modified OPEFB cellulose

Sample	Polymorph	Diffraction angle 2θ (°)				Xc
		1$\bar{1}$0	110	200	040	
Based on	Cellulose I	14.8	16.3	22.6	34.5	--
Literature [63-65]	Cellulose II	12.1	19.8	22	--	--
PA-23-24-70	Cellulose I	14.79	15.85	21.59	33.71	85.4
PA-5-3.5-70-D	Cellulose I	14.66	15.97	21.75	33.89	80.7
Blank	Cellulose I	15.29	16.93	22.81	34.42	78.9
PA-45-3.5-70	Cellulose I	14.81	15.76	22.2	34.61	78.4
PA-23-2.5-70	Cellulose I	14.31	15.71	21.68	33.89	77.82
PA-23-3.5-70	Cellulose I	14.81	15.89	21.86	34.16	77.45
	Cellulose II	11.03	19.06		--	
PA-5-3.5-70	Cellulose I	14.87	16.36	22.24	34.23	75.35
	Cellulose II	11.06	19.13		--	
PA-23-1-70	Cellulose I	14.89	16.16	22.53	34.63	75.1
	Cellulose II	12.73	19.16		--	
PA-5-3.5-75	Cellulose I	13.08	~16.3	22.31	35.2	61.7
	Cellulose II	11.94	20.13		--	
PA-5-2.5-75	Cellulose I	14.81	16.38	22.18	34.64	60.8
	Cellulose II	12.57	19.55		--	
PA-5-24-70	Cellulose II	11.1	19.59	22.22	--	53.3
PA-63-1-70	Cellulose I	14.99	16.98	22.48	3476	52.5
PA-5-1-75	Cellulose I	15.11	17.12	22.39	~34.5	42
	Cellulose II	11.06	19.45		--	
PA-5-2.5-70	Cellulose I	14.76	16.28	22.29	33.31	41.6
	Cellulose II	11.05	19.15		--	

6.5   About Crystallinity

In **Figure 6-13** is shown a direct correlation between the crystallinity index and the lateral order index. This means that increase LOI also increase Xc. There are two incongruous data points that belong to samples PA-23-3.5-70 and PA-63-1-70 this is associated with the complexity of the samples. The hydrolysis reaction of sample PA-63-1-70 was stopped due to cellulose was being decomposed.
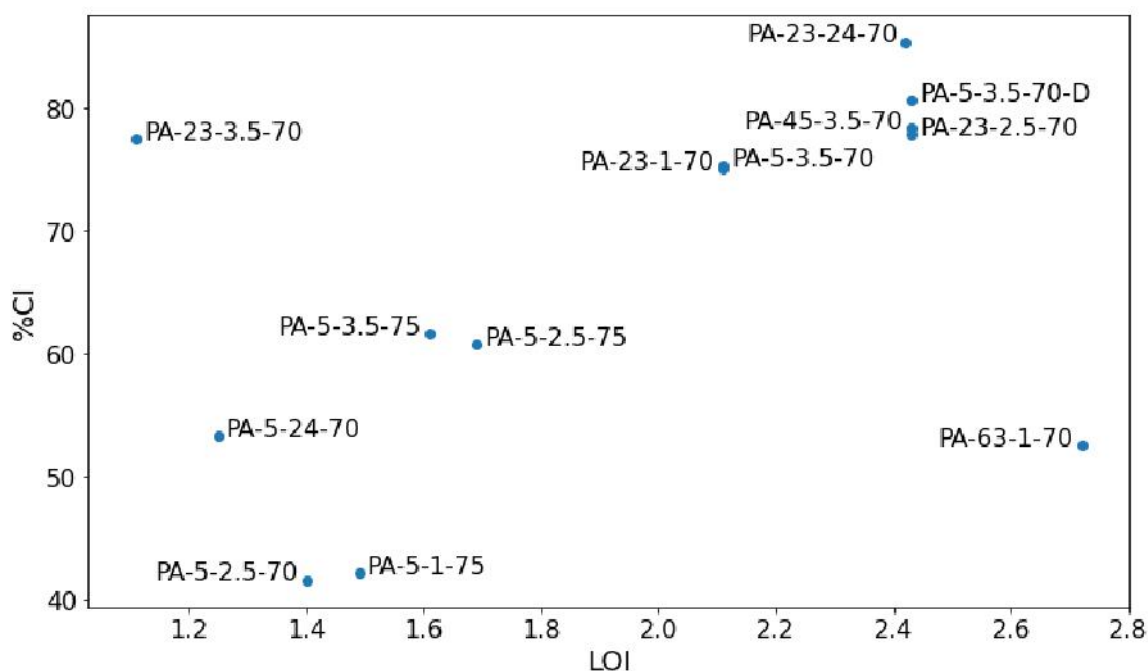
Figure 6-13. Xc vs. LOI

6.6   Morphology Study - Imaging analysis

6.6.1   Stereomicroscopy

Stereomicrographs were taken of OPEFB cellulose fibers shown in **Figure 6-14**, where fibrous material can be seen on the micro scale. The samples were prepared like a microscope sample and were visualized for 2 min. The purpose of visualizing an amplified 3D image of the OPEFB cellulose were to appreciate the change in the morphology of the reference sample and continue with the following experiments. The scale proposed for all stereomicrographs were 200 µm and the average width of particles was calculated based on 15 randomly chosen particles from stereomicrographs. The sample of **Figure 6-14 (a)** correspond to unhydrolyzed OPEFB cellulose that allows us to set a reference standard to see how acid hydrolysis influences on cellulose

morphology. The fiber size of OPEFB is in the range of 200 ~ 700 μm. For the hydrolyzed OPEFB cellulose does not present a visual difference between the **Figure 6-14 (b)** sonicated sample and **Figure 6-14 (c)** no sonicated sample. The length of OPEFB cellulose was distributed in the range of 50 ~ 500 μm. In sonicated sample there are material smaller than in no sonicated sample but this result is circumstantial because it depends on how the sample has been prepared and which part of the sample is observed. In this set of stereomicrographs is possible observe fibers much larger than the scale. The fibers look thick and long but after hydrolysis treatment with phosphoric acid the thickness suffered a large decrease and the length shows a small decrease with respect to thickness. The experimental conditions to acid hydrolysis were 65% H_3PO_4 in a ratio of 1:100 g/mL, for 40 min under magnetic stirring 500 rpm at 60°C.
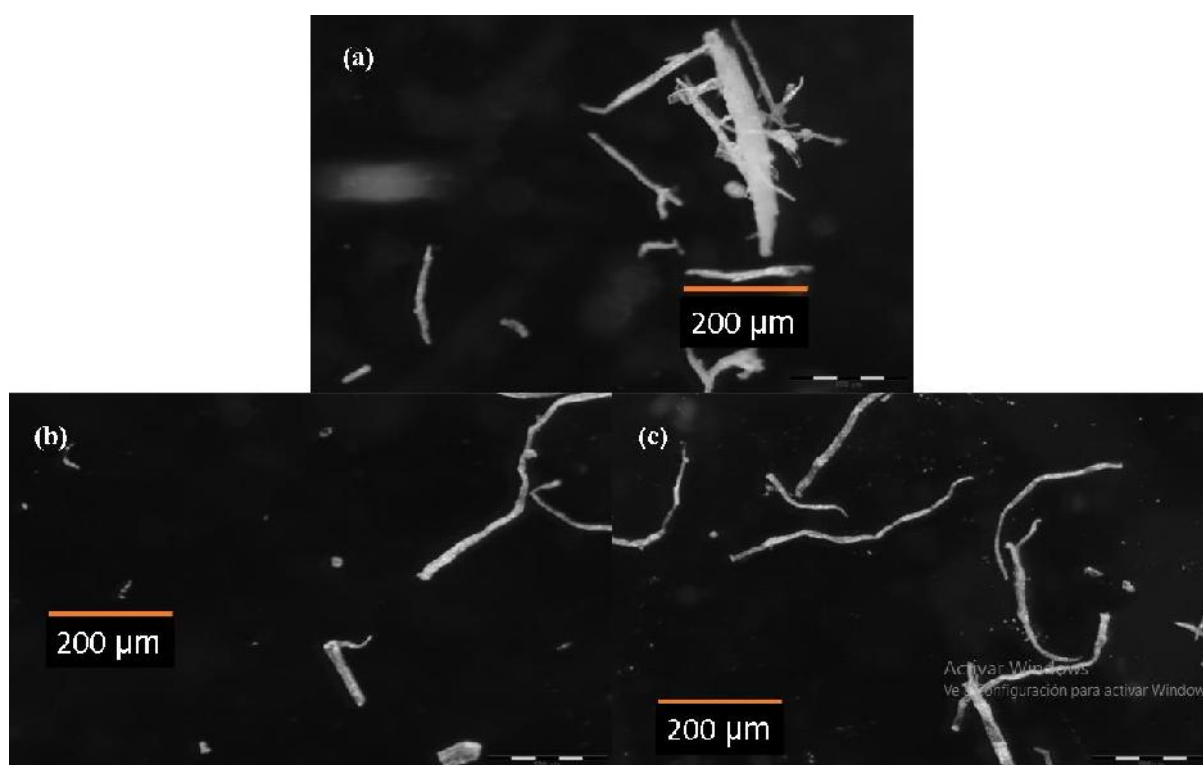
Figure 6-14. Stereomicrographs OPEFB cellulose (a) unhydrolyzed, hydrolyzed (b)sonicated, and (c) no sonicated

6.6.2 SEM Analysis

The Scanning Electron Microscopy characterization technique were used to visualize the differences between the surface morphologies of the cellulose samples isolated from OPEFB biomass. Before to prepare SEM samples, all experiments were sonicated to avoid agglomeration of particles. For sample observation, all samples were put on carbon tape mounted on an aluminum

stub. The morphological analysis is shown according to the temperature at which each experiment was carried out. In this section, it pretends to do a correlation between temperature and particle size if it is possible. The average width of particles was calculated based on 15 randomly chosen particles from SEM images.

6.6.2.1 Samples at low temperature

The first images set shown in **Figure 6-15** that were hydrolyzed at 5°C to different times. (PA-5-2.5-70, PA-5-3.5-70, PA-5-24-70) and a sample hydrolyzed during 3.5h at the same temperature but a different quenching process was carried out with DMSO (PA-5-3.5-70-D). The observable results show that the shape and size of particle cellulose varies with the hydrolysis time. For sample PA-5-2.5-70 in **Figure 6-15 (a)** the observed nanocellulose do not have uniform shapes and distribution and the length was distributed in the range of 800 nm or less. Respect to sample PA-5-3.5-70 in **Figure 6-15 (b)** there is round material and its particle size is in the range of 200 ~ 600 nm and for sample PA-5-24-70 in **Figure 6-15 (c)** is possible appreciate nanomaterial until to 50 nm. When comparing the samples PA-3.5-70 in **Figure 6-15 (b)** and PA-3.5-70-D in **Figure 6-15 (d)** is observed that particle size is slightly smaller than for sample where DMSO is used as quenching reagent. In this set sample was achieved CNCs, there is considerable decrement in size after phosphoric acid hydrolysis and there is not fiber presence.
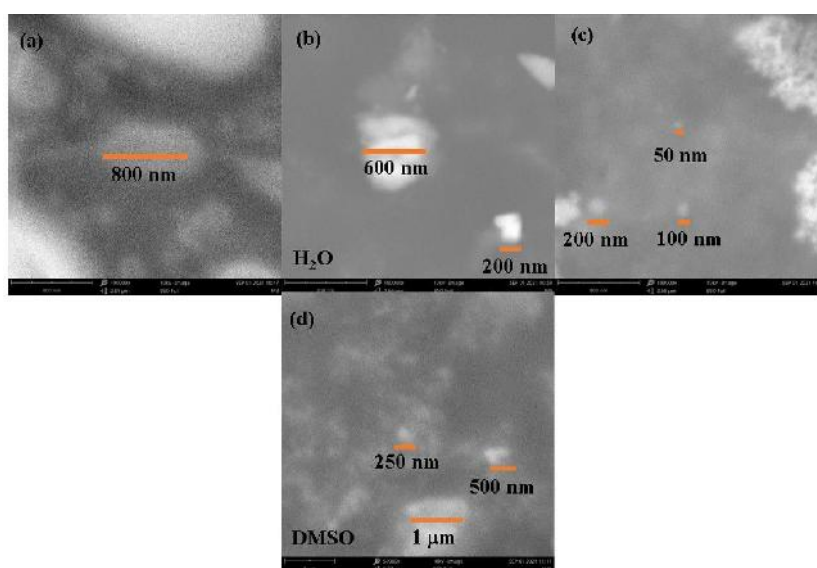
Figure 6-15. SEM micrographs for samples (a) PA-5-2.5-70, (b) PA-5-3.5-70, (c) PA-5-24-70 and (d) PA-5-3.5-70-D

The second micrographs set shown in **Figure 6-16** include the samples PA-5-1-75, PA-5-2.5-75 and PA-5-3.5-75. The evaluated parameters for this samples were the acid concentration and the reaction time. The fibrous material is appreciating for all samples of this set. A remarkable point is for sample PA-5-2.5-75 in **Figure 6-16 (b)** the material is a mixture between microfibrils and round nanospheres. The distribution does not have uniformity and the length fibers are much bigger than micrograph scale proposed (80 µm). Respect to evaluated conditions is possible affirm short reaction times there are not effectiveness even if the acid concentration suffer a slightly increase.
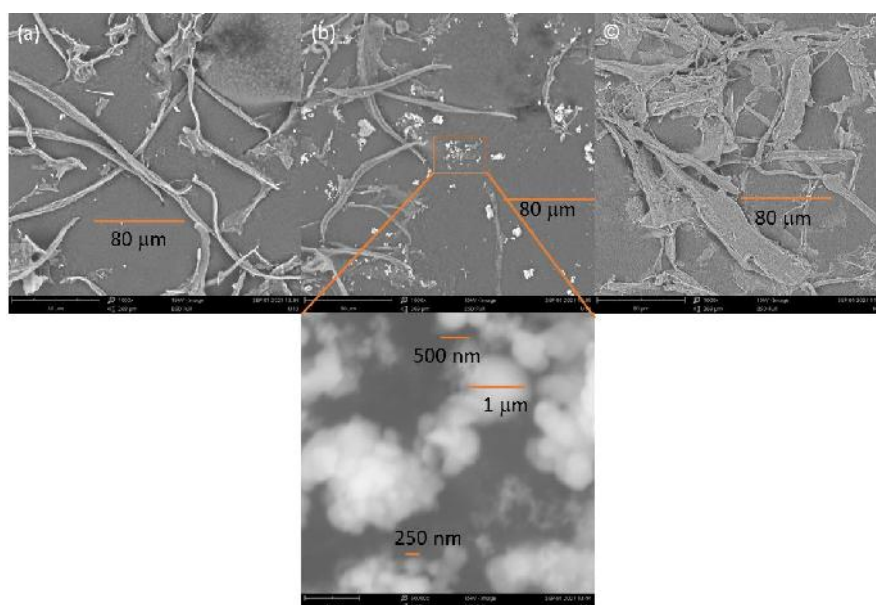
Figure 6-16. SEM micrographs for samples (a) PA-5-1-75, (b) PA-5-2.5-75 and (c) PA-5-3.5-75

6.6.2.2 Samples at room temperature

As shown in **Figure 6-17** include sample that were hydrolyzed at 23°C in a different times. For all samples was achieve the isolation of Microfibrillated Cellulose (MFC). The size particle is in the range [1-100 µm]. The microfibrils do not have uniform distribution. For sample PA-23-1-70 in **Figure 6-17 (a)** only is possible appreciate fibrous material but for samples PA-23-2.5-70 in **Figure 6-17 (b)** and PA-23-3.5-70 in **Figure 6-17 (c)** noticed an intertwined morphology, the nanospheres are seen like nodular agglomerates on their surface of microfibrils. The approximate size oscillates 500nm to nanospheres and >1µm for fibrous material. In sample PA-23-24-70 in **Figure 6-17 (d)** there is only fibrous material between 60µm and 100µm.
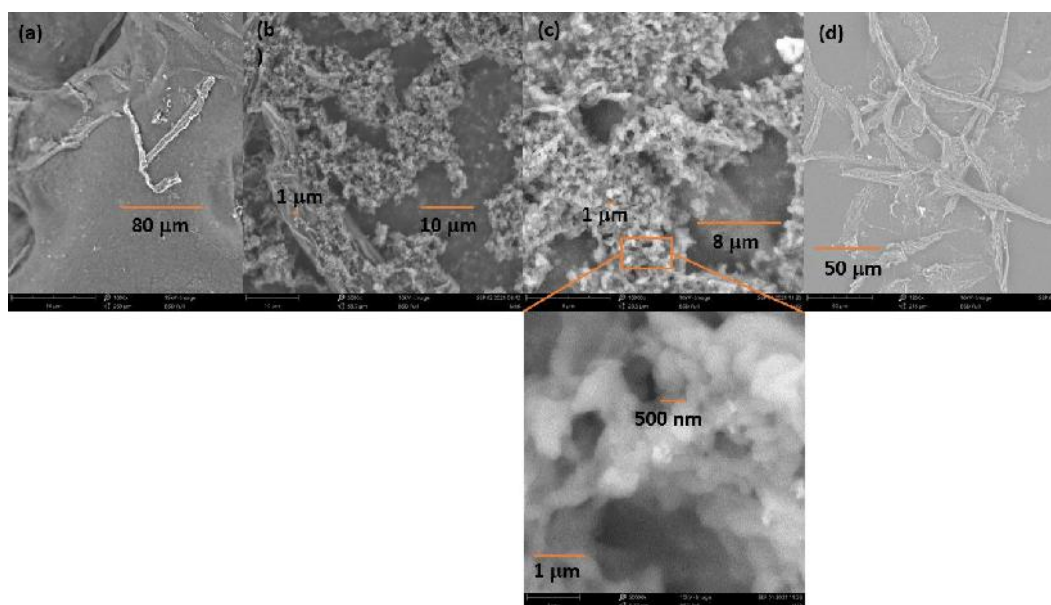
Figure 6-17. SEM micrographs for samples (a) PA-23-1-70, (b) PA-23-2.5-70, (c) PA-23-3.5-70 and (d) PA-23-24-70.

6.6.2.3 Samples at high temperatures

Two experiments were carried out at high temperatures. For sample PA-45-3.5-70 the experimental procedure for OPEFB cellulose was a phosphoric acid hydrolysis at a concentration of 70% in a ratio 1:50 g/mL, at 45°C for 4 hours. In **Figure 6-18** there is round material ant it particle size is in the range of 200 ~ 500 nm.
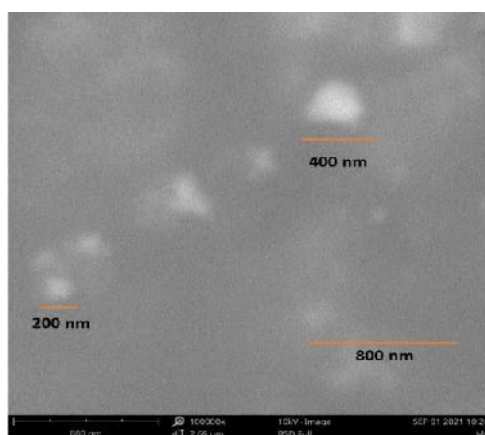
Figure 6-18. SEM micrograph for sample PA-45-3.5-70

The acid hydrolysis of sample PA-63-1-70 was performed at 70% of H_3PO_4 concentration in a ratio 1:50 g/mL during an hour at 63°C. In **Figure 6-19** is possible observe fibrous material in the microscale proposed. For set images to high temperatures, the result is to obtain CNC the best conditions to perform an accurate acid hydrolysis are time and ratio cellulose–acid.
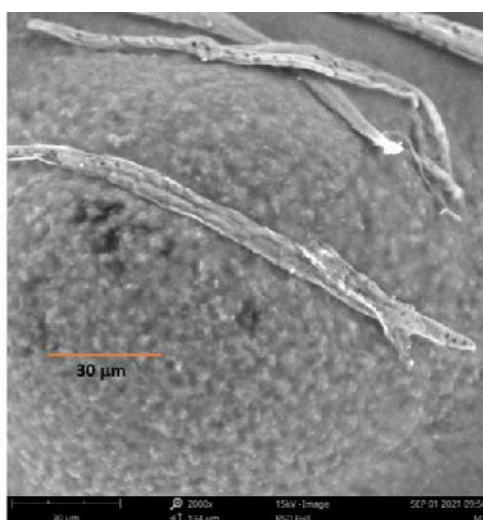
Figure 6-19. SEM micrograph for sample PA-63-1-70

More prominent results about morphology material as well as particle size are in the **Table 6-6**.

Table 6-6. Summarize results of SEM technique for modified OPEFB cellulose

Sample	Approximate size	Fibrous material	Observation
PA-5-2.5-70	> 500nm	NO	Amorphous shape
PA-5-3.5-70	200nm - 600 nm	NO	Round shape
PA-5-24-70	50nm - 200nm	NO	Round shape
PA-5-3.5-70-D	<250nm - 1μm	NO	Round shape
PA-5-1-75	> 80μm	YES	
PA-5-2.5-75	>500nm - >80μm	YES	Sphere and fiber
PA-5-3.5-75	> 80μm	YES	
PA-23-1-70	> 80μm	YES	
PA-23-2.5-70	<500nm - 1μm	YES	Sphere and fiber
PA-23-3.5-70	<500nm - 1μm	YES	Sphere and fiber
PA-23-24-70	60μm - 100μm	YES	
PA-45-3.5-70	200nm - 500nm	NO	Round shape
PA-63-1-70	> 200μm	YES	

6.7   Mechanical Properties

Cellulose and chitosan are polysaccharides with similar structure that is why is very interesting the use of cellulose as a reinforcement of chitosan films. The difference between them is their functional group at the C-2 position. In the case of cellulose has a secondary hydroxyl group while the chitosan has a primary amine [67]. In order to explore the purpose of OPEFB cellulose at the industrial field, we prepared films based on a chitosan – Modified OPEFB cellulose. Films containing 2% w/v chitosan, and 2% w/v OPEFB cellulose hydrolyzed with phosphoric acid at different conditions. All film samples were prepared by solution casting using acetic acid 2% (30ml to each sample) and molding to produce films with uniform width.

6.7.1   Chitosan - Modified OPEFB Cellulose

Based on previous results on this work, the modified OPEFB Cellulose samples comprises both crystalline and amorphous regions. The influence of different types of modified OPEFB cellulose on the mechanical properties of chitosan (CH) was studied comparing Young's modulus, %elongation and tensile strength of each films. To provide more consistent results, each test was repeated five times under the same conditions and present the average of them. Also shown the standard deviation to get more reliable results. Pictures of films are shown in **Figure 6-20.**

Figure 6-20. Films of chitosan - OPEFB cellulose

To study mechanical properties 15 films were prepared. The film labeled as CH did not have cellulose which served in this work as a reference sample to see if the presence of modified OPEFB cellulose improves or not the properties of the chitosan film. In parallel way, was prepared a sample using OPEFB cellulose without hydrolyzing to evaluate the effectiveness of crystalline nanoparticles and cellulose microfibrils over cellulose. The rest of the films were made with OPEFB cellulose hydrolyzed at different conditions using H_3PO_4. All the films were made with the same procedure, despite this, not all samples had a homogeneous distribution as expected. The following **Table 6-7** presents information on the distribution of cellulose on chitosan films.

Table 6-7. Dispersion of chitosan- modified OPEFB cellulose

Chitosan - Modified OPEFB cellulose			
Homogeneous		Heterogeneous	
N° Exp.	Sample	N° Exp.	Sample
1	CH	9	CH:PA-5-1-75
2	CH:PA-5-2.5-70	10	CH:PA-5-2.5-75
3	CH:PA-5-3.5-70	11	CH:PA-5-3.5-75
4	CH:PA-5-24-70	12	CH:PA-23-1-70
5	CH:PA-5-3.5-70-D	13	CH: PA-23-3.5-70
6	CH:PA-23-2.5-70		
7	CH:PA-23-24-70		
8	CH:PA-45-3.5-70		
14	CH:PA-63-1-70		
15	CH:T		

For the samples CH: PA-5-1-75, CH: PA-5-2.5-75, CH: PA-5-3.5-75, CH: PA-23-1-70 and PA-23-3.5-70 the results of mechanical properties were not exposed due to have a heterogeneous distribution which subsequently promotes agglomeration. The hydrogen bonding between functional groups of chitosan and cellulose are important to obtain an appropriate fiber-matrix interfacial adhesion. In addition, the homogeneity of composite film depends of many parameters like shape, size, orientation of cellulose that determine the optimal composite film conditions [68]. That is why that heterogeneous distribution samples are less reliable and no adequate evaluation of the data can be done. So, the analysis was done only over homogeneous films.

6.7.1.1 Stress-Strain Curve

In the present work a typical stress–strain curve for chitosan - modified OPEFB cellulose film looks as is shown the **Figure 6-21**. The curve behavior belongs to ductile polymer compared to chitosan only content film so, based on behavior and the other realized tests is possible affirm that the material of our films corresponds to semi crystalline polymer. According to [69,70] for chitosan- OPEFB cellulose films the results are expected a relatively high Young's modulus and

elastic modulus, but with higher fracture toughness respect to films that only contain chitosan. This curve has an elastic region and a plastic region. Polymers have a non-linear zone which is the non-linear viscoelastic in this region is possible determine the yield strength. In plastic region the point of major interest is tensile strength which correspond to maximum applied stress and the applied stress to fracture is another interest point [71]. From the stress-strain curve of each homogeneous sample could be determined Young's modulus, the yield strength, the tensile strength and % elongation that reveal some mechanical properties of this modified OPEFB cellulose proposed as green filler material.
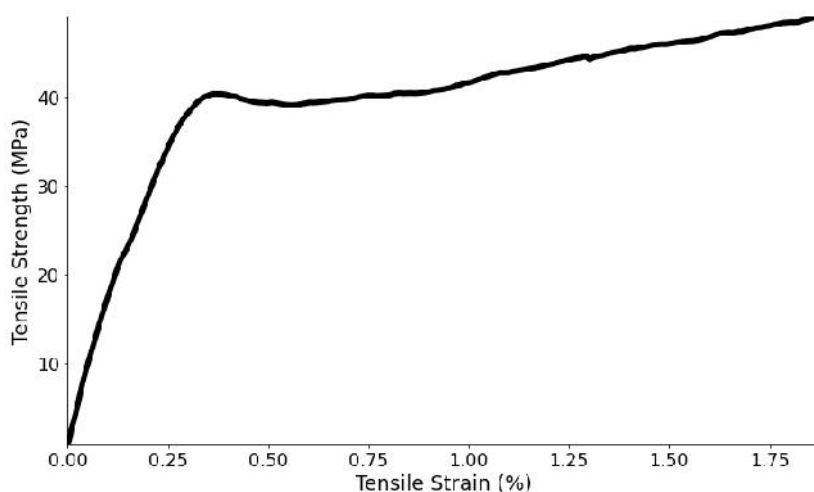
Figure 6-21. Typical stress–strain curve for chitosan - modified OPEFB cellulose films

The final properties are strictly connected to the source of cellulose. In the present work, obtained cellulose are polymorph type I or type II and a mixture of both polymorphs. These two forms of cellulose have dissimilar arrangement in their polysaccharide chains also present different sizes on them elementary cells, and they have different degree of crystallinity which cellulose I present higher crystallinity over cellulose II [67].

6.7.1.2 Young's modulus

The Young's modulus graph of Chitosan- Modified cellulose films at different conditions of phosphoric acid hydrolysis for OPEFB cellulose are plotted in **Figure 6-22**. An important fact to notice is in dependence of label sample, they have different reaction conditions, types of polymorphs and crystalline percentage. Look at section 4 in **Table 6-2.**
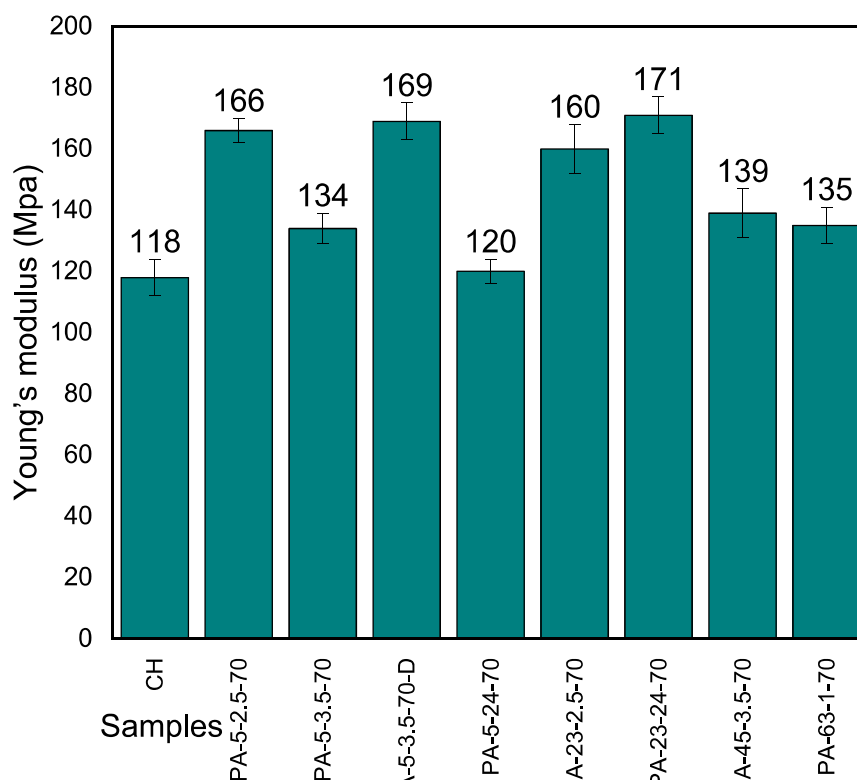
Figure 6-22. Young's modulus graph of Chitosan- Modified cellulose films

All films show an improvement with the incorporation of 2 wt. % modified cellulose concentration. The percentage of cellulose added to chitosan is optimal according the literature review [72-74]. The referential film labeled as CH which belong to chitosan film without OPEFB cellulose has Young's modulus of 118±6 MPa and for sample CH:PA-5-24-70 has a value of 120±4 MPa in this case could not appreciate an increment comparing the films. Sample PA-5-3.5-70 has 134±5 MPa and increase in 14%, the sample CH:PA-63-1-70 has a 135±6 MPa for Young's modules with an increment of 15%, sample CH:PA-45-1-70 suffer an increment of 18% and has a value of 139±8 MPa, sample PA-23-2.5-70 has 160±8 MPa and an addition of 36% respect blank, sample CH:PA-5-2.5-70 has 166±4 MPa and rise in 42%, for sample CH:PA-5-3.5-70-D has 169±6 MPa and a 43% higher Young's modulus and 171±6 MPa for sample PA-23-24-70 with an increment of 45%. Based on increment of Young's modulus the sample more effective were sample PA-23-24-70 and PA-5-3.5-70-D. The increment of Young's modulus for the samples that contain OPEFB cellulose is expected in dependence of the polymorph present. The samples where only exist cellulose type I have a higher value that samples where exist a mixture of polymorphs.

The reactions conditions were different in all aspects. So, based only on the conditions for the samples there is not a trend that help to find a critical reaction condition with the purpose of improving Young's modulus. Respect with Xc, sample PA-23-24-70 has 85.4% and sample CH:PA-5-3.5-70-D has 80.7% and present only cellulose polymorph type I. Is possible affirm that high crystalline percentage in sample increase the Young's modulus.

6.7.1.3 Stress to break

The Stress to break graph of Chitosan- Modified cellulose films at different conditions of phosphoric acid hydrolysis for OPEFB cellulose are plotted in **Figure 6-23**. Each modified cellulose sample has different reaction conditions, types of polymorphs and crystalline percentage.
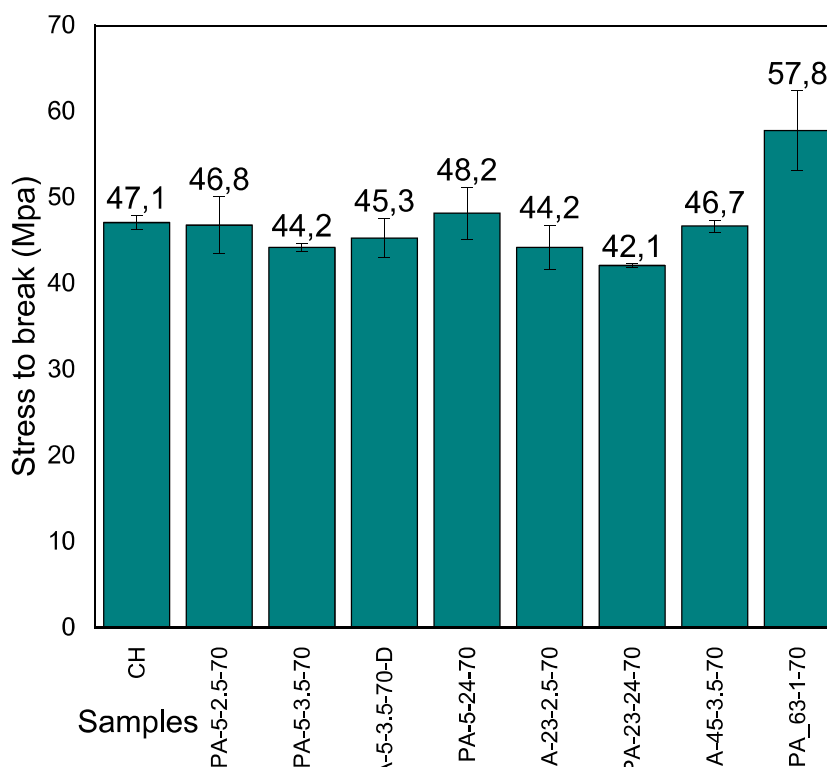

Figure 6-23. Tensile strength curve of Chitosan- Modified cellulose films

For the stress to break analysis all homogeneous samples were compared between them and there is not a significant change. This means that is possible to increase the Young's modulus and not affect the stress to break The blank sample CH, the tensile strength is 47.1 ± 0.8 MPa. Sample

CH:PA-5-24-70 present a slightly high value of 48.2 ± 3.0 MPa but with error range affirm that behavior of sample CH:PA-5-24-70 is equal to blank sample. For samples CH:PA-5-2.5-70, CH:PA-45-3.5-70, CH:PA-23-1-70 and CH:PA-5-3.5-70-D which stress to break have values of 46.8 ±3.3 MPa, 46.7 ± 0.7 MPa, 44.2 ± 2.6 MPa and 45.3 ± 2.3 MPa respectively, is possible notice that behavior is similar, they have the same value as blank sample. The sample PA-5-3.5-70 has 44.2 ± 0.5 MPa and shows a slightly decrement of 2.18% sample CH:PA-23-24-70 has 42.1 ± 0.2 MPa with a decrement of 8.73%. The sample CH:PA-63-1-70 has 57.8 ± 4.6 and increment of 15,21% compared with the chitosan film, one aspect to emphasize is that this sample present only polymorph type I but a lower crystallinity index respect to the others obtained samples. Also, for sample CH:PA-63-1-70 which is an outlier value respect with the reported for the rest of evaluated films the difference is it size particle >200 μm. About the results is possible affirm that the reactions conditions do not affect the stress to break. Respect to morphology of OPEFB cellulose is possible affirm that the size of fiber has an influence over this value. As no significant variation is observed in the results of the chitosan-OPEFB cellulose films with respect to the blank, is difficult assured a tendency with the crystallinity index or the type of polymorph present.

6.7.1.4 Elongation

The % Elongation graph of Chitosan- Modified cellulose films at different conditions of phosphoric acid hydrolysis for OPEFB cellulose are plotted in **Figure 6-24**. Each modified cellulose sample has different reaction conditions, types of polymorphs and crystalline percentage.
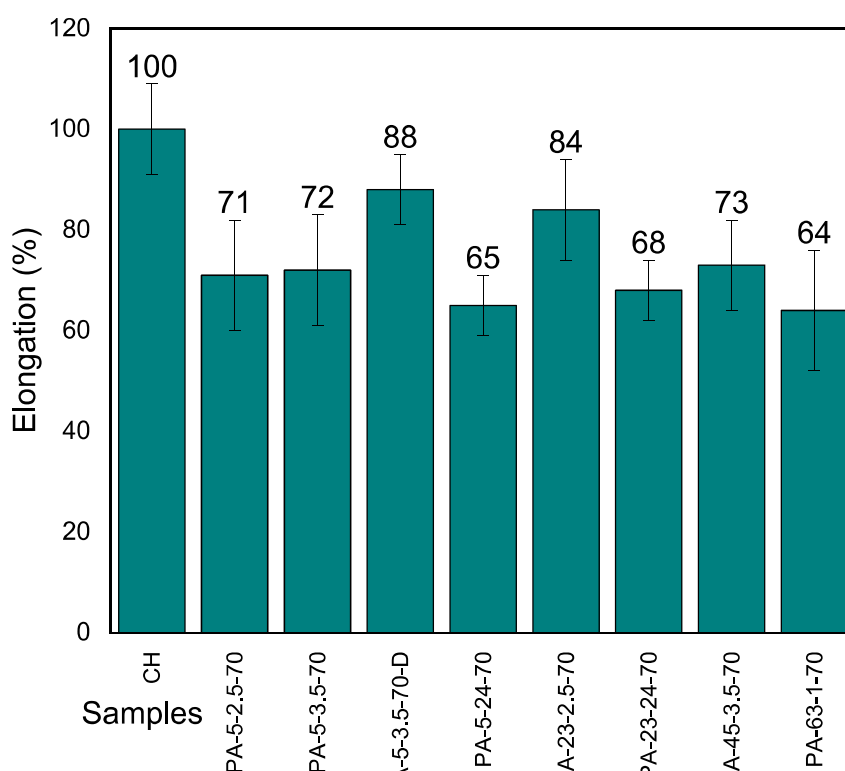
Figure 6-24. %Elongation graph of Chitosan- Modified cellulose films

The elongation values show a decrement with the incorporation of 2 wt. % modified cellulose concentration. The sample CH which is the reference point due to the film only contain chitosan has an elongation percentage of 100 ± 9 %. For the samples CH:PA-5-3.5-70-D and CH:PA-23-2.5-70 notice that the elongation is similar to the blank, their values are 88 ± 7 % and 84 ± 10 % respectively. The rest of samples decrease according the reference. For sample CH:PA-45-3.5-70 is 73 ± 9 %, for sample CH:PA-5-3.5-70 is 72 ± 11 %, sample CH:PA-5-2.5-70 is 71 ± 11%, for sample CH:PA-23-24-70 its value is 68 ± 6%, sample CH:PA-5-24-70 is 65 ± 6 % and 64 ± 12 % for sample CH:PA-63-1-70. The elongation percentage show a decrement in the sample films up to 21.98%. According with data samples that has a minor elongation are samples CH:PA-23-24-70 and CH:PA-5-24-70. This behavior with the integration of modified OPEFB cellulose into chitosan matrix resulted in a lack of interactions that decreases the ability to transmit stress, promoting premature rupture at the stress concentration points, in the interface. There is not a previsible reaction conditions. Respect to morphology, the sample CH:PA-5-24-70 which present a decrement in 21.98% respect to the chitosan film, it size particle is in the range of 50-200 nm and present a round shape, while for sample CH:PA-23-24-70 decrement is observed in 18.69%

respect the chitosan film it size particle is in the range of 60-100 µm and is a fibrous material. This means that based on this data, is not possible stablish a tendency between morphological characteristics and % Elongation. About Xc for sample CH:PA-5-24-70 has a value of 53.3% and present only cellulose type II, for sample CH:PA-23-24-70 Xc is 85.4% and present only cellulose type I so there is no a visible tendency based on crystallinity and type of polymorph.

All results about mechanical properties are condensed in **Annex 2**. For samples is important mention that for acid hydrolysis is used 70% H_3PO_4 for homogeneous films. The results demonstrated that modified OPEFB cellulose films in a ratio 2:100 g/ml increase mechanical properties. Moreover, factors such as the reaction conditions, % crystallinity, type of cellulose polymorph and the morphology of modified OPEFB cellulose (CNC, MFC, MCC and AC) and interactions between the polymeric matrix and the hydrolyzed cellulose modified the properties of the films achieving in a general way major rigidity. About the Young's modulus data of the chitosan film, raising up to 45%. The results also illustrated that elongation percentage has lower values compared to the pure chitosan film. The %Elongation data show a decrement in the sample films up to 21.98%. Based on the results obtained, it can be ensured that the samples CH:PA-5-3.5-70-D, CH:PA-23-2.5-70 and CH:PA-23-24-70have a good balance of mechanical properties, so it will be analyzed what characteristics they have in common. About reaction conditions do not observe a critical parameter. About the Xc all samples have high values respect to other samples tested. The values of crystallinity are 80.7%, 77,82% and 85.4% and fact to notice is for all of this set of samples the only polymorph present is cellulose type I. Respect to morphology, the sample CH:PA-5-3.5-70-D has a size particle approximately <250nm (CNC) and without fiber presence, for sample CH:PA-23-2.5-70 was obtained nanoparticles and fibrous material (CNC, MFC) and for sample CH:PA-23-24-70 only obtained fibrous material (MFC). According with the comparison of samples the worst balance between mechanical properties belongs to sample CH:PA-5-24-70. This sample has Xc of 53.3 and only present cellulose type II. This fact affirms that the arrangement of polysaccharide chains in cellulose is a determining factor over the mechanical properties. With cellulose type I is expected an increment on stiffness comparing with cellulose type II. The size sample of CH:PA-5-24-70 is 50-200nm (CNC) and do not have the presence of fibrous material. So, is possible affirm that the increase of their Young's modulus is

not dependent of size and shape of cellulose. By increasing the stiffness of our chitosan-OPEFB cellulose films, the elongation is decreased.

6.7.1.5   Correlation of mechanical results

In **Figure 6-25** is shown an inversely proportional correlation between Young's modulus and % Elongation. This means that if Young's modulus increase, the elongation of the material decrease. A high value for Young's modulus show resistance to the deformation. Based on this information the samples PA-5-3.5-70-D, PA-23-24-70, PA23-2.5-70 and PA-5-2.5-70 are more notorious this trend. About the reaction conditions for the samples there is not a critical condition. As atypical values of the prepared samples we have sample PA-5-24-70. An increase in Young's modulus is expected a decrease in elongation.
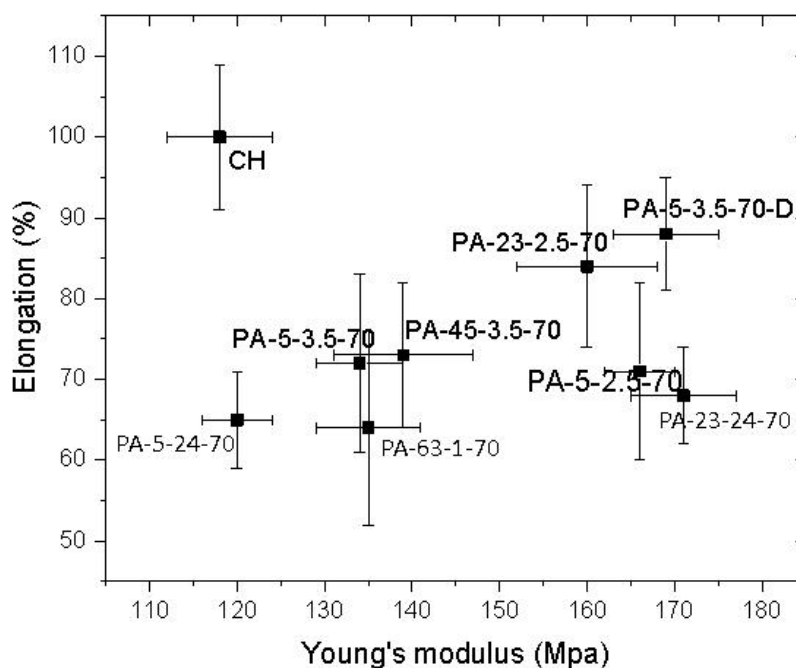
Figure 6-25. %Elongation vs. Young's modulus graph of Chitosan- Modified cellulose films

The **Figure 6-26** shows the behavior between crystallinity and Young's modulus. There is possible affirm that exist a direct correlation between these parameters. This means that if crystallinity index increase, the Young's modulus of the material decrease. Is important remark that the arrangement of polysaccharide chains from cellulose affect the crystallinity. For chitosan-OPEFB cellulose films in which the obtained cellulose contains only polymorph type I present higher

values of crystallinity and higher values of Young´s modulus comparing with films where cellulose contains polymorph type II. The exception in this set sample is film labeled as CH:PA-63-1-70 because has low Xc value and contains only cellulose type I. This fact can be explained by the size particle. The fibrous material (MFC) is in the range of 60-100 μm due to the conditions of acid hydrolysis. In the case of CH:PA-5-2.5-70. Respect to direct correlation there is one exception that is the film CH:PA-5-2.5-70 which present high Young's modulus but the worst crystalline index. The idea that size and morphology affect this property can be backed with this sample due to CNC obtained were >500nm size particle.
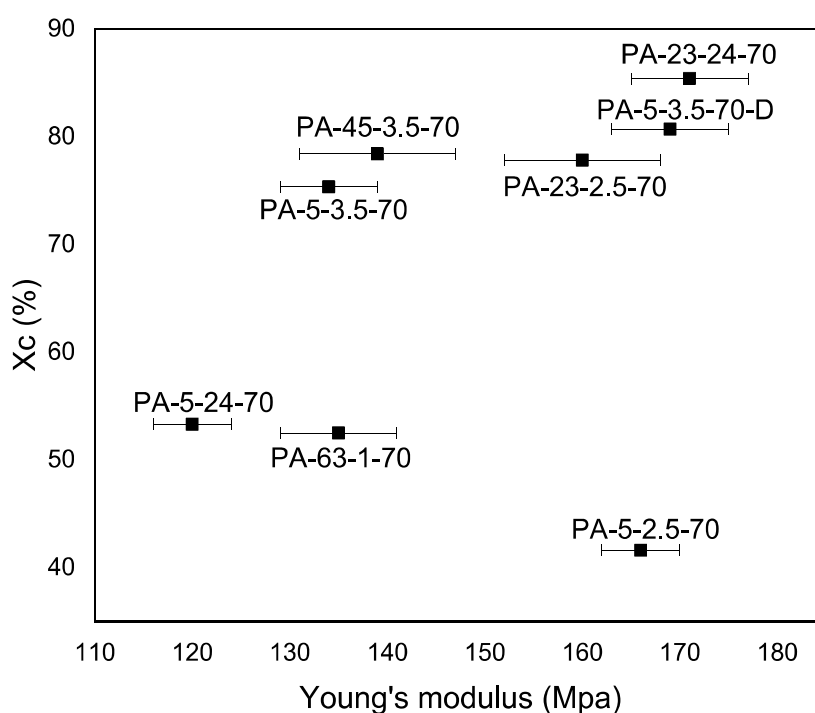
Figure 6-26. Xc vs. Young's modulus graph of Chitosan- Modified cellulose films

In **Figure 6-27** is shown the influence of OPEFB cellulose morphology over Young's modulus. The morphology like unique parameter is not critical to stablish a trend with the Young´s modulus. For relatively high Young's modulus values belongs to samples PA-5-3.5-70-D, PA-5-2.5-70 present CNC, PA23-2.5-70 for both CNC and MFC particles and PA-23-24-70 for MFC. So, there is not a tendency based only on them size and shape. To do an appropriate analysis of the morphology are necessary more homogeneous films of chitosan-OPEFB cellulose which present MFC and a mixture of CNC and MFC.
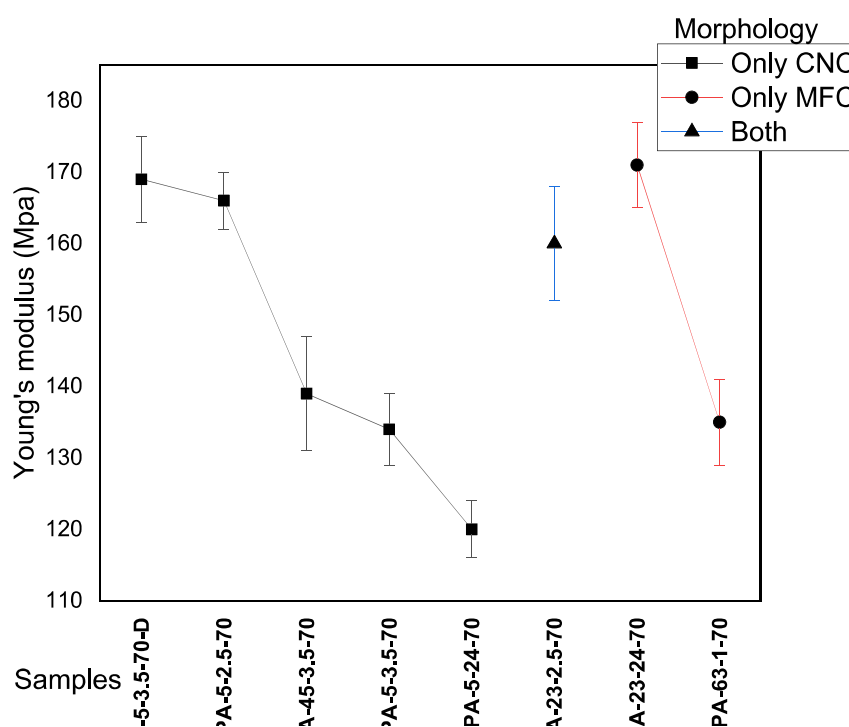
Figure 6-27Influence of morphology on Young's modulus

6.8   Suspension Stability

The stability of suspended cellulose depends of interaction between the dispersed phase and the dispersion phase. The cellulose is an amphiphilic polymer, this means that have hydrophilic and a hydrophobic region due to the presence of crystalline cellulose or amorphous cellulose. In general way, the suspension stability depends on many factors like geometry, size, shape and surface density [75]. In the case of use water (pH around 6) as dispersion media There is an acidic character that favors adsorb OH- group and influence in their colloidal stability by the presence of a double electrical layer under their surface, resulting from the dissociation of different functional groups, such as carboxylic [76]. The modified OPEFB cellulose was diluted to particle concentration of 2 % w/v using distilled water. The suspension was placed in test tubes at room temperature of 23°C. All experiments were monitored in an interval of ten minutes as shown in **Figure 6-28**. The purpose of realize this experiment is to appreciate if exist an effect on the stability of the regenerated cellulose suspensions due to morphological structure of cellulose.   The CNC suspensions obtained from OPEFB cellulose were homogeneous at t = 0 min so a colloidal suspension was observed in all samples. The regenerated cellulose but not stable. So, the

sedimentation process starts at 10 minutes approximately. The results suggest that ultrasonication process helps to particle distribution. An in a future work this factor will be taking in account.
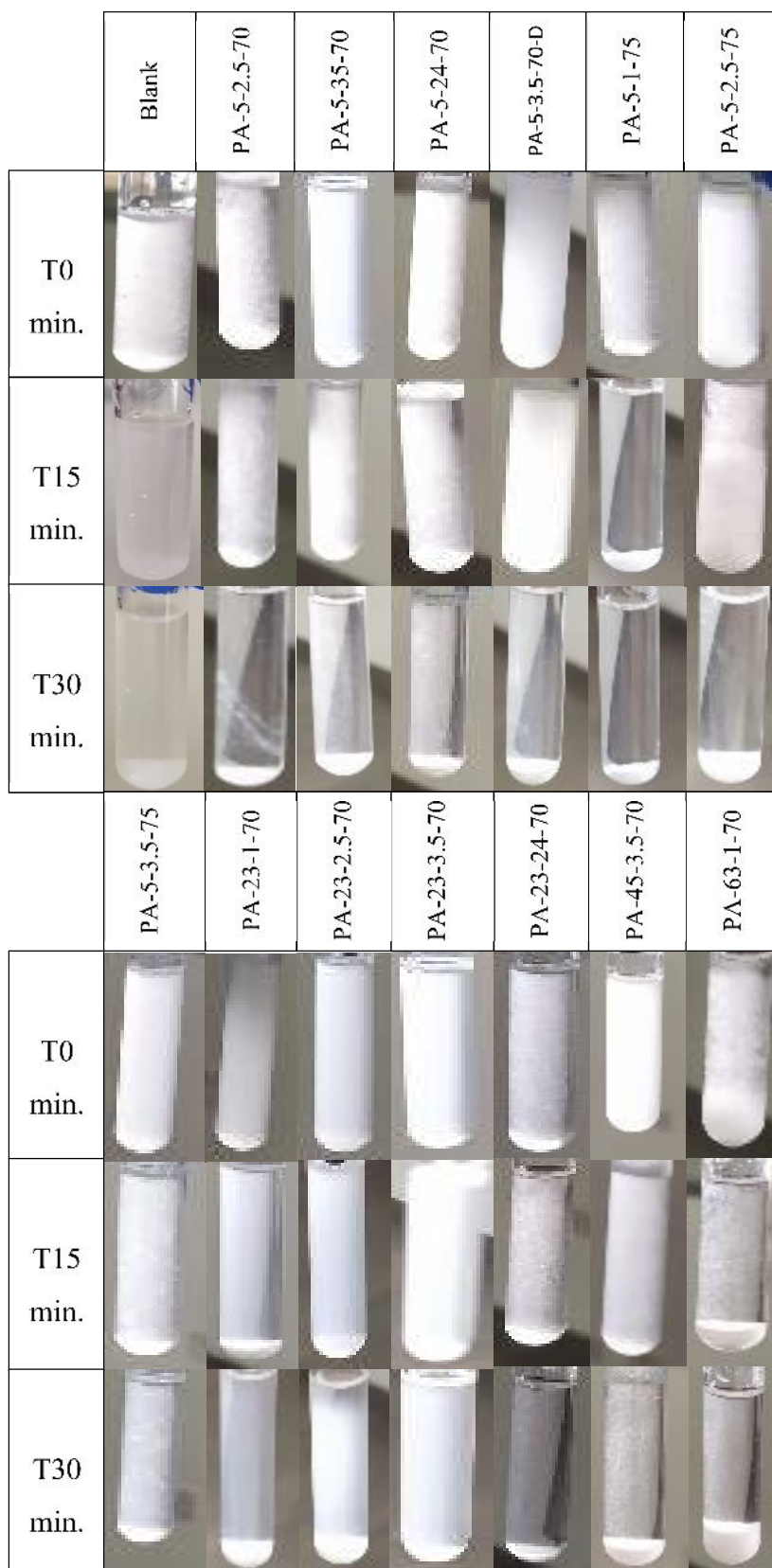

Figure 6-28. Photographs of suspension stability of CNC from OPEFB

7   CONCLUSIONS AND RECOMMENDATIONS

The methodology suggests for all experiments of this work present a percentage yield range [33-81%] depending the reaction conditions. The temperature is a critical condition; it was evidenced by sample PA-63-1-70 which is OPEFB cellulose hydrolyzed at 63 °C during an hour. The reaction was stopped because the sample was decomposing by the acid. The %yield was only of 33.1%. In a general way, it can be affirming that the suitable temperature for obtaining CNCs is at room temperature (23 °C). The samples PA-23-1-70, PA-23-2.5-70, PA-23-3.5-70 obtained the % crystalline index range in [75.1-77.8%] with a yield reaction of 81%. The reaction time is also a critical condition in a good performance. The sample PA-23-24-70 was hydrolyzed during 24hours and the %crystallinity was improving respect to unhydrolyzed cellulose. The quenching reagents were evaluated in samples PA-5-3.5-70 and PA-5-3.5-70-D. They have equal reaction conditions but the difference in %yield is approximately in 10%. The use of DMSO for quenching process reduce yield but according to the crystalline index, it improves approximately in 6%. Also is important report that in the sample PA-5-3.5-70-D (quenched with DMSO) only has cellulose polymorph type I, while the sample PA-5-3.5-70 which is quenched with water shows both polymorphs. This fact suggests do a study of other crystallization methods in order to improve the quality of the cellulose.

The morphology structure was confirmed with Scanning Electron Microscopy. The work of this thesis shows a promising green route to isolate MFC, MCC and CNCs from OPEFB cellulose. Depending on what is needed, certain conditions are proposed for phosphoric acid hydrolysis. In the case of CNCs the best conditions results in the sample PA-5-3.5-70-D with a Xc of 80.7 and a yield of 79.59%. For the samples PA-5-2.5-70, PA-23- 2.5-70 and PA-23-3.5-70 where obtained MFCs and CNCs. This suggest to explore a better sonication technique that the used in the present work. With the ATR- FTIR characterization technique was possible affirm that phosphoric acid hydrolysis has a successful performance on modified OPEFB cellulose due to was possible assign all fundamental peaks of cellulose, showing that cellulose was pure because does not have the peaks that correspond to lignin and hemicellulose.

With X-ray Powder Diffractometer was possible determinate the crystalline percentage from all samples including a sample of unhydrolyzed cellulose that serve as reference. There were two

samples (PA-23-24-70 and PA-5-3.5-70-D) that improve Xc from starting material. In a parallel way this technique allows assign the cellulose polymorph type. The samples present polymorph types I (PA-23-24-70, PA-5-3.5-70-D, Blank, PA-45-3.5-70, PA-23-2.5-70 and PA-63-1-70), II only sample PA-5-24-70 and the rest of samples present both polymorphs. The Xc was directly correlated with LOI calculated in ATR-FTIR technique. For final, to study the mechanical performance of modified OPEFB cellulose, films were made on a ratio 1:1 chitosan-modified OPEFB cellulose in a dry basis. There were five films that cannot evaluate the mechanical properties due to the dispersion of cellulose was heterogeneous. This fact suggests a study about the optimal concentration for modified OPEFB cellulose. For the rest of samples, it was shown that by incorporating MFC, MCC and CNCs in chitosan-based films the Young's modulus increase for all films and them % Elongation decrease. The optimal properties of chitosan-OPEFB cellulose films will be achieved in dependance of desired application. Further studies are recommended for a sustainable application such as green filler.

8   BIBLIOGRAPHY

[1] Toral, M. C. T., & Espinoza, F. G. A. (2018). Análisis correlacional entre la producción del aceite de palma, sus exportaciones y su contribución al PIB agrícola durante el período 2010-2017. Dominio de las Ciencias, 4(4), 270-283.

[2] Medina, J. D. C., Magalhães, A. I., Zamora, H. D., & Melo, J. D. Q. (2019). Oil palm cultivation and production in South America: status and perspectives. Biofuels, Bioproducts and Biorefining. doi:10.1002/bbb.2013

[3] Instituto nacional de estadísticas y censos INEC–ESPAC, Ministerio de Agricultura y Ganadería (MAG). 2019. https://www.agricultura.gob.ec/agricultura-la-base-de-la-economia-y-la-alimentacion/

[4] Rafidah, D. & Mohamed, Ainun Zuriyati & Hazwani, H.A. & Ibrahim, Rushdan & Luqman Chuah, Abdullah & Adnan, Sharmiza & M. Tahir, Paridah & Jalaluddin, H.. (2017). Characterisation of pulp and paper manufactured from oil palm empty fruit bunches and kenaf fibres. Pertanika Journal of Tropical Agricultural Science. 40. 449-457.

[5] Zainal, S. H., Mohd, N. H. h, Suhaili, N., Anuar, F. H., Lazim, A. M., & Othaman, R. (2020). Preparation of Cellulose-based Hydrogel: A Review. Journal of Materials Research and Technology. doi:10.1016/j.jmrt.2020.12.012

[6] Hasanin, M., El-Henawy, A., Eisa, W. H., El-Saied, H., & Sameeh, M. (2019). Nano-amino acid cellulose derivatives: Eco-synthesis, characterization, and antimicrobial properties. International Journal of Biological Macromolecules. doi:10.1016/j.ijbiomac.2019.04.

[7] Bezerra, R. D. S., Teixeira, P. R. S., Teixeira, A. S. N. M., Eiras, C., Osajima, J. A., & Filho, E. C. S. (2015). Chemical Functionalization of Cellulosic Materials — Main Reactions and Applications in the Contaminants Removal of Aqueous Medium. Cellulose - Fundamental Aspects and Current Trends. doi:10.5772/61431

[8] Berg, J. M.; Tymoczko, J. L.; Stryer, L.; Gregory, J.; Gatto, J. Biochemistry, 7th ed.; 2012.

[9] Poletto, M., Pistor, V., & J., A. (2013). Structural Characteristics and Thermal Properties of Native Cellulose. Cellulose - Fundamental Aspects. https://doi.org/10.5772/50452

[10] Quiroz Castañeda, Rosa & Folch-Mallol, Jorge. (2013). Degradation of Lignocellulosic Biomass - Techniques, Applications and Commercialization Sustainable Degradation of Lignocellulosic Biomass - Techniques, Applications and Commercialization.

[11] Hildén L, Johansson G. Recent developments on cellulases and carbohydrate-binding modules with cellulose affinity. Biotechnology Letters. 2004;26(22):1683-93.

[12] Kunusa, W. R., Isa, I., Laliyo, L. A. R., & Iyabu, H. (2018). FTIR, XRD and SEM Analysis of Microcrystalline Cellulose (MCC) Fibers from Corncorbs in Alkaline Treatment. Journal of Physics: Conference Series, 1028(1). https://doi.org/10.1088/1742-6596/1028/1/012199

[13] Karimi, K., & Taherzadeh, M. J. (2016). A critical review of analytical methods in pretreatment of lignocelluloses: Composition, imaging, and crystallinity. Bioresource Technology, 200, 1008–1018. doi:10.1016/j.biortech.2015.11.

[14] Kristiani, A; Abimanyu, H; Setiawan, A H; Sudiyarmanto and Aulia, F (2013). Effect of pretreatment process by using diluted acid to characteristic of oil palm's frond. Energy Procedia, 32: 183-189

[15] Medina, J D C; Woiciechowsk, A; Filho, A Z; Noseda, M D; Kaur, B S and Soccol, C R (2015). Lignin preparation from oil palm empty fruit bunches by sequential acid/alkaline treatment - a biorefinery approach. Bioresource Technology, 194: 172-178.

[16] Zheng, Y; Pan, Z, Zhang, R (2009). Overview of biomass pretreatment for cellulosic ethanol production. International J. Agricultural and Biological Engineering, 2: 51-68.

[17] Rabemanolontsoa, H., Saka, S (2016). Various pretreatment of lignocellulosics. Bioresource Technology, 199: 83-91.

[18] Singha, A. S., & Guleria, A. (2014). Chemical modification of cellulosic biopolymer and its use in removal of heavy metal ions from wastewater. International Journal of Biological Macromolecules, 67, 409–417. doi:10.1016/j.ijbiomac.2014.03.046

[19] Zhang, G., Zhang, L., Deng, H., & Sun, P. (2011). Preparation and characterization of sodium carboxymethyl cellulose from cotton stalk using microwave heating. Journal of Chemical Technology & Biotechnology, 86(4), 584–589. doi:10.1002/jctb.2556

[20] Huang, A., Peng, X., Geng, L., Zhang, L., Huang, K., Chen, B., … Kuang, T. (2018). Electrospun poly (butylene succinate)/cellulose nanocrystals bio-nanocomposite scaffolds for tissue engineering: Preparation, characterization and in vitro evaluation. Polymer Testing. doi:10.1016/j.polymertesting.2018.08.027

[21] Yang, Y., Chen, Z., Zhang, J., Wang, G., Zhang, R., & Suo, D. (2019). Preparation and Applications of the Cellulose Nanocrystal. International Journal of Polymer Science, 2019, 1–10. doi:10.1155/2019/1767028

[22] Burhani, D., & Septevani, A. A. (2018). Isolation of nanocellulose from oil palm empty fruit bunches using strong acid hydrolysis.

[23] Pandi, N., Sonawane, S. H., & Anand Kishore, K. (2021). Synthesis of cellulose nanocrystals (CNCs) from cotton using ultrasound-assisted acid hydrolysis. Ultrasonics Sonochemistry, 70, 105353. doi:10.1016/j.ultsonch.2020.105353

[24] Sofla, M. R. K., Brown, R. J., Tsuzuki, T., & Rainey, T. J. (2016). A comparison of cellulose nanocrystals and cellulose nanofibres extracted from bagasse using acid and ball milling methods. Advances in Natural Sciences: Nanoscience and Nanotechnology, 7(3), 035004. doi:10.1088/2043-6262/7/3/035004

[25] Jonoobi, M., Oladi, R., Davoudpour, Y., Oksman, K., Dufresne, A., Hamzeh, Y., Davoodi, R., 2015. Different preparation methods and properties of nanostructured cellulose from various natural resources and residues: a review. Cellulose 22, 935–969. https://doi.org/10.1007/s10570-015-0551-0.

[26] Frost, B. A., & Foster, E. J. (2020). Isolation of thermally stable cellulose nanocrystals from spent coffee grounds via phosphoric acid hydrolysis. Journal of Renewable Materials, 8(2), 187.

[27] Kassem, I., Kassab, Z., Khouloud, M., Sehaqui, H., Bouhfid, R., Jacquemin, J., … Achaby, M. E. L. (2020). Phosphoric acid-mediated green preparation of regenerated cellulose spheres and their use for all-cellulose cross-linked superabsorbent hydrogels. International Journal of Biological Macromolecules. doi:10.1016/j.ijbiomac.2020.06.

[28] Wang, Z., Yao, Z., Zhou, J., He, M., Jiang, Q., Li, S., ... & Luo, S. (2019). Isolation and characterization of cellulose nanocrystals from pueraria root residue. International journal of biological macromolecules, 129, 1081-1089.

[29] Jia, X., Chen, Y., Shi, C., Ye, Y., Wang, P., Zeng, X., & Wu, T. (2013). Preparation and Characterization of Cellulose Regenerated from Phosphoric Acid. Journal of Agricultural and Food Chemistry, 61(50), 12405–12414. doi:10.1021/jf4042358

[30] Stuart, B. H. (2004). Infrared spectroscopy: fundamentals and applications. John Wiley & Sons.

 [31] Minnes, R., Nissinmann, M., Maizels, Y., Gerlitz, G., Katzir, A., & Raichlin, Y. (2017). Using Attenuated Total Reflection–Fourier Transform Infra-Red (ATR-FTIR) spectroscopy to distinguish between melanoma cells with a different metastatic potential. Scientific reports, 7(1), 1-7.

[32] Schuttlefield, J. D., & Grassian, V. H. (2008). ATR–FTIR spectroscopy in the undergraduate chemistry laboratory. Part I: fundamentals and examples. Journal of chemical education, 85(2), 279.

[33] Maghfiroh, A. M. R. (2020). Evaluation of thermal testing and X-ray diffraction of Ka0, 5Na0, 5NbO3. Gravity: Jurnal Ilmiah Penelitian dan Pembelajaran Fisika, 6(1).

[34] Cullity, B.; Stock, S., Elements of X-ray Diffraction, Third Edition; Prentice-Hall: 2001.

[35] Nothnagle, P., Chambers, W. & Davidson, M. Introduction to Stereomicroscopy. MicroscopyU https://www.microscopyu.com/techniques/stereomicroscopy/introduction-to-stereomicroscopy (2013).

[36] DE ESTEREOSCÓPIOS, C. L. A. S. E. S., & DE BOLSILLO, E. D. L. O. EL ESTEREOSCOPIO. Fundamentos de FOTOGRAMETRÍA para imagenes de contacto y digitales, 105.

[37] Vernon-Parry, K. D. (2000). Scanning electron microscopy: an introduction. III-Vs Review, 13(4), 40-44.

[38] Leonard, D. N.; Chandler, G. W.; Seraphin, S., Scanning Electron Microscopy; American Cancer Society: 2012, pp 1–16.

[39] Inkson, B., 2 - Scanning electron microscopy (SEM) and transmission electron microscopy (TEM) for materials characterization; Hübschen, G.,Altpeter, I., Tschuncky, R., Herrmann, H.-G., Eds.; Woodhead Publishing: 2016, pp 17 –43.

[40] Davis, J. R. (Ed.). (2004). Tensile testing. ASM international.

[41] Modenbach, A.A. & Nokes, Sue. (2014). Effects of sodium hydroxide pretreatment on structural components of biomass. Transactions of the ASABE. 57. 1187-1198. 10.13031/trans.56.10046.

[42] Johar, N., Ahmad, I., & Dufresne, A. (2012). Extraction, preparation and characterization of cellulose fibres and nanocrystals from rice husk. Industrial Crops and Products, 37(1), 93–99. doi:10.1016/j.indcrop.2011.12.0

[43] Dungani, R., Owolabi, A. F., Saurabh, C. K., Abdul Khalil, H. P. S., Tahir, P. M., Hazwan, C. I. C. M., … Aditiawati, P. (2016). Preparation and Fundamental Characterization of Cellulose Nanocrystal from Oil Palm Fronds Biomass. Journal of Polymers and the Environment, 25(3), 692–700. doi:10.1007/s10924-016-0854-8

[44] Jonoobi, M., Oladi, R., Davoudpour, Y., Oksman, K., Dufresne, A., Hamzeh, Y., & Davoodi, R. (2015). Different preparation methods and properties of nanostructured cellulose from various natural resources and residues: a review. Cellulose, 22(2), 935-969.

[45] Wang, T., & Zhao, Y. (2021). Optimization of bleaching process for cellulose extraction from apple and kale pomace and evaluation of their potentials as film forming materials. Carbohydrate Polymers, 253, 117225. doi:10.1016/j.carbpol.2020.1172

[46] Haerunnisa, A., Ramadhan, D., Putra, H. A. Y., Afiifah, N., Devita, R., Rahayu, S., & Nandiyanto, A. B. D. (2020). Synthesis of Crystalline Nanocellulose by Various Methods. Arabian Journal of Chemical and Environmental Research, 7(2), 94-125.

[47] Tang, Y., Shen, X., Zhang, J., Guo, D., Kong, F., & Zhang, N. (2015). Extraction of cellulose nano-crystals from old corrugated container fiber using phosphoric acid and enzymatic hydrolysis followed by sonication. Carbohydrate Polymers, 125, 360–366. doi:10.1016/j.carbpol.2015.02.063

[48] Kontturi, E. (2018). Preparation of Cellulose Nanocrystals: Background, Conventions and New Developments. In Nanocellulose and Sustainability (pp. 27-44). CRC Press.

[49] Banerjee, M., Saraswatula, S., Williams, A., & Brettmann, B. (2020). Effect of Purification Methods on Commercially Available Cellulose Nanocrystal Properties and TEMPO Oxidation. Processes, 8(6), 698. doi:10.3390/pr8060698

[50] Khoshkava, V., & Kamal, M. R. (2014). Effect of drying conditions on cellulose nanocrystal (CNC) agglomerate porosity and dispersibility in polymer nanocomposites. Powder Technology, 261, 288–298. doi:10.1016/j.powtec.2014.04.0

[51] Hänninen, A., Sarlin, E., Lyyra, I., Salpavaara, T., Kellomäki, M., & Tuukkanen, S. (2018). Nanocellulose and chitosan based films as low cost, green piezoelectric materials. Carbohydrate Polymers. doi:10.1016/j.carbpol.2018.09.001

[52] Yadav, M., Behera, K., Chang, Y.-H., & Chiu, F.-C. (2020). Cellulose Nanocrystal Reinforced Chitosan Based UV Barrier Composite Films for Sustainable Packaging. Polymers, 12(1), 202. doi:10.3390/polym12010202

[53] Segal, L., Creely, J. J., Martin, A. E., & Conrad, C. M. (1959). An Empirical Method for Estimating the Degree of Crystallinity of Native Cellulose Using the X-Ray Diffractometer. Textile Research Journal, 29(10), 786–794. doi:10.1177/004051755902901003

[54] Nazir, M. S., Wahjoedi, B. A., Yussof, A. W., & Abdullah, M. A. (2013). Eco-friendly extraction and characterization of cellulose from oil palm empty fruit bunches. BioResources, 8(2), 2161-2172

[55] Ching, Y. C., & Ng, T. S. (2014). Effect of preparation conditions on cellulose from oil palm empty fruit bunch fiber. BioResources, 9(4), 6373-6385.

[56] Boukir, A., Fellak, S., & Doumenq, P. (2019). Structural characterization of Argania spinosa Moroccan wooden artifacts during natural degradation progress using infrared spectroscopy (ATR-FTIR) and X-Ray diffraction (XRD). Heliyon, 5(9), e02477. doi:10.1016/j.heliyon.2019.e02477

[57] Ling, Z., Wang, T., Makarem, M., Santiago Cintrón, M., Cheng, H. N., Kang, X., … French, A. D. (2019). Effects of ball milling on the structure of cotton cellulose. Cellulose. doi:10.1007/s10570-018-02230-x

[58] Santos, S. M., Carbajo, J. M., Quintana, E., Ibarra, D., Gomez, N., Ladero, M., … Villar, J. C. (2015). Characterization of purified bacterial cellulose focused on its use on paper restoration. Carbohydrate Polymers, 116, 173–181. doi:10.1016/j.carbpol.2014.03.064

[59] Zghari, Badreddine & L., Hajji & Boukir, Abdellatif. (2018). Effect of Moist and Dry Heat Weathering Conditions on Cellulose Degradation of Historical Manuscripts exposed to Accelerated Ageing: 13C NMR and FTIR Spectroscopy as a non-Invasive Monitoring Approach. Journal of Materials and Environmental Sciences. 9. 641-654. 10.26872/jmes.2018.9.2.71.

[60] Ismail, H., Edyham, M. R., & Wirjosentono, B. (2002). Bamboo fibre filled natural rubber composites: the effects of filler loading and bonding agent. Polymer Testing, 21(2), 139–144. doi:10.1016/s0142-9418(01)00060-5

[61] Nelson, M. L., & O'Connor, R. T. (1964). Relation of certain infrared bands to cellulose crystallinity and crystal lattice type. Part II. A new infrared ratio for estimation of crystallinity in celluloses I and II. Journal of Applied Polymer Science, 8(3), 1325–1341. doi:10.1002/app.1964.070080323

[62] Oh, S. Y., Yoo, D. I., Shin, Y., & Seo, G. (2005). FTIR analysis of cellulose treated with sodium hydroxide and carbon dioxide. Carbohydrate Research, 340(3), 417–428. doi:10.1016/j.carres.2004.11.027

[63] Nam, S., French, A. D., Condon, B. D., & Concha, M. (2016). Segal crystallinity index revisited by the simulation of X-ray diffraction patterns of cotton cellulose Iβ and cellulose II. Carbohydrate Polymers, 135, 1–9. doi:10.1016/j.carbpol.2015.08.035

[64] Valencia, L., Arumughan, V., Jalvo, B., Maria, H. J., Thomas, S., & Mathew, A. P. (2019). Nanolignocellulose extracted from environmentally undesired Prosopis juliflora. ACS Omega, 4(2), 4330-4338

[65] Rongpipi, S., Ye, D., Gomez, E. D., & Gomez, E. W. (2019). Progress and opportunities in the characterization of cellulose–an important regulator of cell wall growth and mechanics. Frontiers in plant science, 9, 1894.

[66] Ishak, W. H. W., Rosli, N. A., & Ahmad, I. (2020). Influence of amorphous cellulose on mechanical, thermal, and hydrolytic degradation of poly (lactic acid) biocomposites. Scientific Reports, 10(1), 1-13

[67] Grzạbka-Zasadzińska, A., Smułek, W., Kaczorek, E., & Borysiak, S. (2017). Chitosan biocomposites with enzymatically produced nanocrystalline cellulose. Polymer Composites, 39, E448–E456. doi:10.1002/pc.24552

[68] Abdul Khalil, H. P. S., Davoudpour, Y., Islam, M. N., Mustapha, A., Sudesh, K., Dungani, R., & Jawaid, M. (2014). Production and modification of nanofibrillated cellulose using various mechanical processes: A review. Carbohydrate Polymers, 99, 649–665. doi:10.1016/j.carbpol.2013.08.069

[69] H.P.S, A. K., Saurabh, C. K., A.S., A., Nurul Fazita, M. R., Syakir, M. I., Davoudpour, Y., … Dungani, R. (2016). A review on chitosan-cellulose blends and nanocellulose reinforced chitosan biocomposites: Properties and their applications. Carbohydrate Polymers, 150, 216–226. doi:10.1016/j.carbpol.2016.05.028

[70] Xiong Chang, X., Mujawar Mubarak, N., Ali Mazari, S., Sattar Jatoi, A., Ahmad, A., Khalid, M., … Nizamuddin, S. (2021). A review on the properties and applications of chitosan, cellulose and deep eutectic solvent in green chemistry. Journal of Industrial and Engineering Chemistry. doi:10.1016/j.jiec.2021.08.033

[71] Physical, Thermal, and Mechanical Properties of Polymers. (2015). Biosurfaces, 329–344. doi:10.1002/9781118950623.app1

[72] Wan Ishak, W.H., Rosli, N.A. & Ahmad, I. Influence of amorphous cellulose on mechanical, thermal, and hydrolytic degradation of poly(lactic acid) biocomposites. Sci Rep 10, 11342 (2020). https://doi.org/10.1038/s41598-020-68274-x

[73] Arianita, A., Cahyaningtyas, Amalia, B., Pudjiastuti, W., Melanie, S., Fauzia, V., & Imawan, C. (2019). Effect of glutaraldehyde to the mechanical properties of chitosan/nanocellulose. Journal of Physics: Conference Series, 1317, 012045. doi:10.1088/1742-6596/1317/1/012045

[74] Talebi, H., Ghasemi, F. A., & Ashori, A. (2021). The effect of nanocellulose on mechanical and physical properties of chitosan-based biocomposites. Journal of Elastomers & Plastics, 00952443211017169.

[75] Stygar, Marina. (2020). Colloidal Stability of Cellulose Suspensions. 10.5772/intechopen.94490.

[76] Li, M. C., Wu, Q., Song, K., Lee, S., Qing, Y., & Wu, Y. (2015). Cellulose nanoparticles: structure–morphology–rheology relationships. ACS Sustainable Chemistry & Engineering, 3(5), 821-832.

9 ANNEXES

Annex 1.
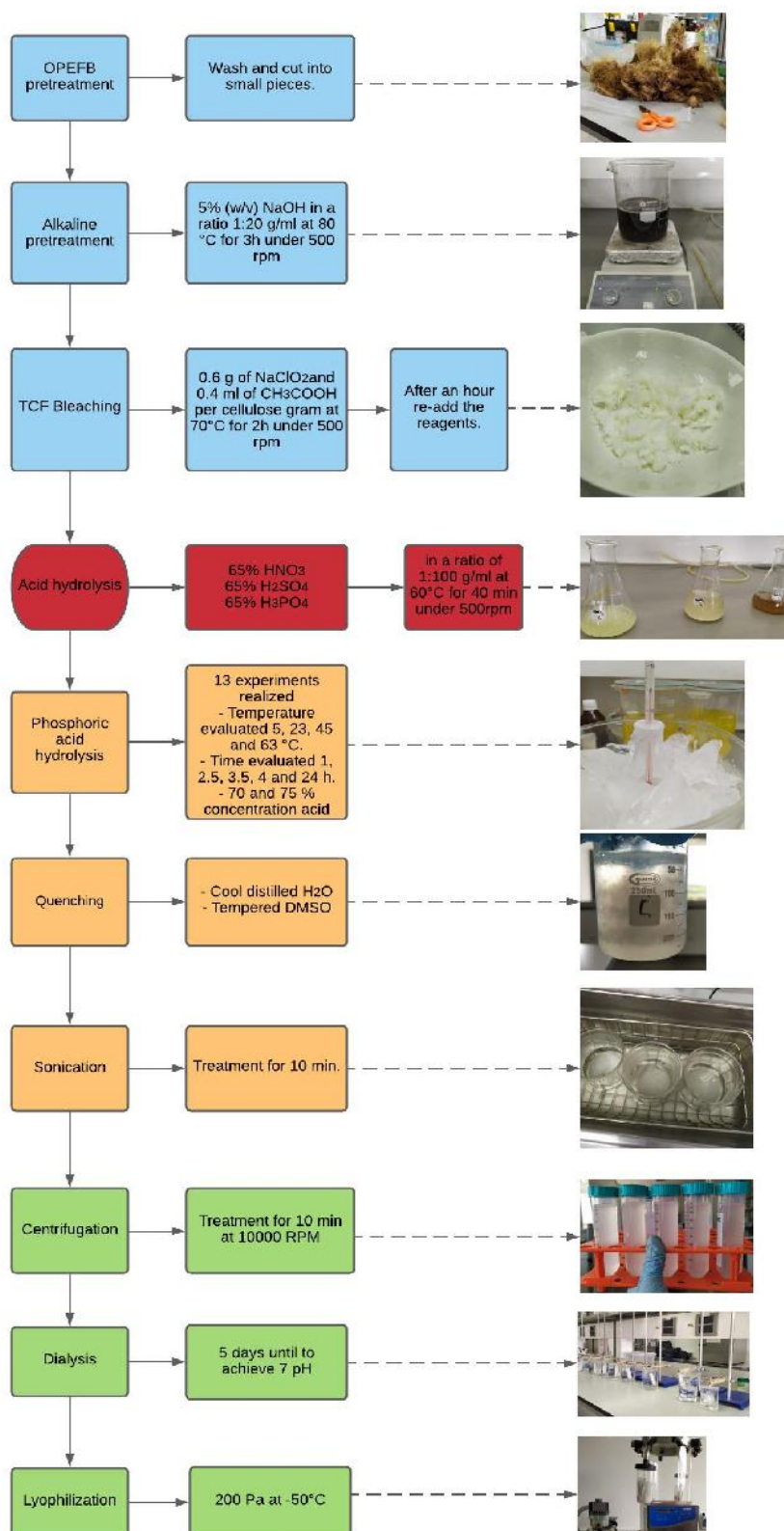
Annex 1. General scheme

Annex 2.

Annex 2. Mechanical properties Chitosan - Modified OPEFB Cellulose

Sample	Mechanical Properties			
	Young's modulus (MPa)	Yield Strength (MPa)	Tensile Strength (MPa)	Elongation (%)
CH	118 ± 6	28.6 ± 3.7	47.1 ± 0.8	100 ± 9
CH:T	133 ± 4	40.3 ± 1.7	38.3 ± 1.6	73 ± 5
CH:PA-5-2.5-70	166 ± 4	40.7 ± 1.0	46.8 ±3.3	71 ± 11
CH:PA-5-3.5-70	134 ± 5	41.2 ± 1.8	44.2 ± 0.5	72 ± 11
CH:PA-5-24-70	120 ± 4	50.0 ± 4.2	48.2 ± 3.0	65 ± 6
CH:PA-5-3.5-70-D	169 ± 6	36.3 ± 0.7	45.3 ± 2.3	88 ± 7
CH:PA-23-2.5-70	160 ± 8	38.0 ± 1.3	44.2 ± 2.6	84 ± 10
CH:PA-23-24-70	171 ± 6	42.8 ± 1	42.1 ± 0.2	68 ± 6
CH:PA-45-3.5-70	139 ± 8	43.9 ± 0.5	46.7 ± 0.7	73 ± 9
CH:PA-63-1-70	135 ± 6	43.0 ± 1.0	57.8 ± 4.6	64 ± 12